Supporting Information for the Manuscript Entitled

(Co)polymerization of (-)-Menthide and β-Butyrolactone with Yttrium-bis(phenolates): Tuning Material Properties of Sustainable Polyesters

Friederike Adams,[a] Thomas M. Pehl,[a] Moritz Kränzlein,[a] Sebastian A. Kernbichl,[a] Jia-Jhen Kang,[b] Christine M. Papadakis[b] and Bernhard Rieger[a,*]

[a.] *WACKER-Chair of Macromolecular Chemistry, Catalysis Research Center, Department of Chemistry, Technical University of Munich, Lichtenbergstr. 4, 85748 Garching (Germany)*
[b.] *Soft Matter Physics Group, Physics Department, Technical University of Munich, James-Franck Str. 1, 85748 Garching (Germany)*

Table of Contents

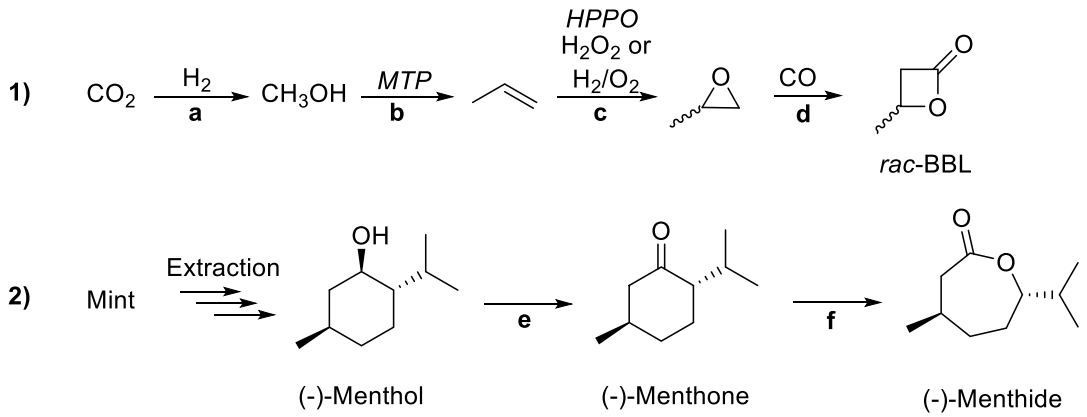

Scheme S1: 1) Synthesis of rac-BBL: a) Catalytic hydrogenative conversion of carbon dioxide to methanol[1]; b) Methanol-to-propylene(MTP)-process[2]; c) Epoxidation of propylene (e.g. HPPO-process)[3-6]; d) Ring expansion of propylene oxide[7-8]. 2) Synthesis of (-)-menthide: e) Oxidation of (-)-menthol[9]; f) Baeyer-Villiger-oxidation[10-11]

1) Experimental section

Materials, Methods and Characterization of Polymer-Samples:

All reactions were carried out under argon atmosphere using standard Schlenk or glovebox techniques. All glassware was heat dried under vacuum prior to use. Unless otherwise stated, all chemicals were purchased from Sigma-Aldrich, Acros Organics, or ABCR and used as received. Toluene, thf, diethyl ether, dichloromethane and pentane were dried using a MBraun SPS-800 solvent purification system. *Racemic* β-butyrolactone was purchased from Sigma-Aldrich and stirred with barium oxide (1.5 equivalents per amount of butyric, hydroxybutyric and crotonic acids; determined *via* ^{1}H-NMR spectroscopy) for 2 days. After centrifugation, the butyrolactone was dried over calcium hydride and distilled prior to use. (-)-Menthide was synthesized according to literature[10-11] and further purified *via* double sublimation.

The precursor complexes $Y(CH_2TMS)_3(thf)_2$ and $Y(bdsa)_3(thf)_2$,[12] the 2-methoxyethylamino-bis(phenolate) ligand[13], $[(ONOO)^{tBu}Y(CH_2TMS)(thf)]$[14] and complexes **1**[15], **2**[16], **3**[17] and **4**[18] were prepared according to literature procedure.

NMR spectra were recorded on a Bruker AVIII-300, AVIII-400 and AVIII-500 Cryo spectrometer. Unless otherwise stated, ^{1}H- and ^{13}C-NMR spectroscopic chemical shifts δ are reported in ppm. δ (^{1}H) is calibrated to the residual proton signal, δ (^{13}C) to the carbon signal of the solvent. Deuterated solvents were obtained from Sigma-Aldrich and dried over 3 Å molecular sieves.

Elemental analysis was measured at the Laboratory for Microanalysis at the Institute of Inorganic Chemistry at the Technische Universität München.

GC-MS analysis was performed using a 7890B GC System from Agilent Technologies equipped with a 30 m HP-5MS UI column (ID = 0.25mm, film = 0.25 µm) and a 5977A mass selective detector from Agilent Technologies. Helium (5.0) was used as carrier gas.

Molecular weights and polydispersities of PHB and polydispersities of all copolymers were measured *via* size-exclusion chromatography (SEC) with samples of 2-3 mg/ml concentration on an PL-SEC 50 Plus from Polymer Laboratories using a refractive index detector (RI detector) with chloroform as eluent relative to polystyrene standards. Absolute molecular weights and polydispersities of PM and the first block of the copolymers were determined by triple detection using two angle light scattering, a refractive index detector and a viscometer (triple detection) in tetrahydrofuran with 0.22 g/L 2,6-di-tert-butyl-4-methylphenol as eluent. The dn/dc was determined *via* SEC measurement of three samples with different concentrations of polymers with various molar masses. It was determined as 0.067 mL/g.

The tacticity determination of PHB was performed by ^{13}C-NMR-spectroscopy at room temperature in $CDCl_3$ on a AVIII 500 Cryo spectrometer with 1000 scans and analyzed according to literature.[19]

DSC measurements were performed on a DSC Q2000 from TA Instruments. It was measured in exo down mode with a heating rate of 10 K/min in a temperature range of -50 °C – 170 °C with samples of 6-9 mg. Three cycles were run per measurement (heating, cooling, heating). The first run is omitted in the graphics.

TGA was measured on a TGA Q5000 from TA Instrument. A high-resolution method was used with a sensitivity of 2.0 and a resolution of 4.0. The sample was heated with a ramp of 10 °C/min to 500 °C under argon.

ESI-MS analytical measurements were performed with acetonitrile solutions on a Varian 500-MS spectrometer in positive ionization mode.

Powder X-ray diffraction measurements were performed using *Bragg-Brentano* geometry in a *PANalytical* Empyrean diffractometer equipped with a *PANalytical* PIXcel 1D detector. X-ray Cu K_α radiation (λ_1 = 1.5406 Å, λ_2 = 1.5444 Å, I_2/I_1 = 0.5) was used for the measurements. K_β radiation is removed with a Ni-filter. Voltage and intensity were 45 kV and 40 mA, respectively. The measurement range was from 5.0° to 40.0° (2θ) with a step size of 0.01313° (2θ) and an acquisition time of 313.65 seconds per step. The scattering angle 2θ is directly measured and can be derived from the generalized *Bragg*-equation $n\lambda = 2dsin\theta$. The obtained diffractograms were Cu-K_α stripped using *Rachingers* method and the background was determined after *Sonneveld* and *Visser* with a bending factor of 8 and a granularity of 82. For comparison reasons, the highest reflex of all diffractograms is normalized to 1.

Small-angle X-ray scattering (SAXS) measurements were performed using a GANESHA 300XL instrument (SAXSLAB, Copenhagen) with a GENIX 3D microfocus X-ray source, point collimation and a 2D Pilatus 300K detector. Cu K_α radiation (λ = 1.54 Å) was used for the measurements, and the instrument was calibrated using silver behenate. Samples were mounted in a cell between two mica windows sealed by an O-ring. The sample-detector distances (SDD) were set as 1051.35, 401.35 and 101.35 mm, and the corresponding exposure times were 1800, 900 and 480 s, respectively. A q-range of 0.005~0.4 $Å^{-1}$ was provided, where q is the momentum transfer, $q = 4\pi sin\theta/\lambda$ (2θ: scattering angle). The scattering intensities collected as 2D images were azimuthally averaged, and the background from the empty sample holder with mica windows was subtracted, taking the transmissions into account. All measurements were carried out at room temperature

In situ IR measurements were performed under argon atmosphere using an ATR IR *MettlerToledo* system.

Stress-strain measurements were performed on a *ZwickRoell* machine with a strain rate of 5 mm/min and analyzed with testXpert II software. Dog-bone shaped specimens were prepared *via* hot molding at 117 °C under vacuum. *Young*'s modulus was determined as the slope between a strain of 0.05% and 0.5%. To proof, whether degradation processes of the samples occur during hot molding, polymers were measured on SEC in chloroform after this procedure. In case of the PHB homopolymer the molar mass and the polydispersity were unaffected (SI, S49). As the molar mass of BAB[3] is measured via NMR-studies, only the polydispersity was considered after hot molding. As the polydispersity was similar before and after polymer processing, no decomposition took place (SI, S50).

Homopolymerization Procedure for rac-BBL

24.9 μmol (1.0 eq.) of the respective catalyst were dissolved in 2 ml of toluene in a screw cap vial in a glove box and 4.98 mmol (200 eq.) racemic β-butyrolactone were added in one portion. After stirring for the stated time at the respective temperature, the reaction was quenched by addition of 1.5 mL deuterated wet chloroform. To determine the conversion, an aliquot (0.4 mL) was taken from this solution and measured by ^{1}H NMR spectroscopy. The polymers were precipitated by addition of the reaction mixtures to methanol (100 ml), and the solution was decanted off. Relative molar masses and molar mass distributions were measured via SEC in chloroform relative to polystyrene.

Homopolymerization Procedure for rac-BBL with in situ Monitoring

All polymerizations with in situ monitoring were performed using a React-IR/MultiMax four-autoclave system (Mettler-Toledo). The 50 mL steel autoclaves were equipped with a diamond window, a mechanic stirring and a heating device. The autoclaves were heated to 130 °C under vacuum prior to polymerization.

For these polymerizations, 24.9 μmol of the respective complex was dissolved in 6.0 mL dichloromethane and transferred to a syringe. 14.9 mmol BBL (600 eq.) was stored in a second syringe. The two syringes were rapidly transported to the reactor using a vial equipped with an injection septum. The autoclave was stored under argon atmosphere at room temperature and the two syringes were transferred into the reactor. An IR spectrum was then taken every 30 seconds. After the given time, an aliquot was taken to determine the conversion via ^{1}H NMR spectroscopy in $CDCl_3$. Chloroform was added to the reaction mixture to stop the polymerization, and the polymer was precipitated by addition of the reaction solution to methanol (100 ml). The solution was decanted off. Relative molar masses and molar mass distribution were measured via SEC in chloroform.

Kinetic Measurements of rac-BBL by Aliquot Method

To a solution of 24.9 μmol of catalyst **4** in 6.0 mL dichloromethane at room temperature, 14.9 mmol BBL (600 eq.) were added in one portion. Aliquots were taken from the reaction solution at regular time intervals and quenched by addition of $CDCl_3$. For each aliquot, the conversion was determined via ^{1}H NMR spectroscopy and the molar mass and polydispersity of the polymer sample were determined by SEC analysis in chloroform relative to polystyrene.

Homopolymerization Procedure for (-)-Menthide

After dissolving the calculated amount of catalyst (24.9 μmol) in toluene (0.5 ml), this solution was added to the respective equivalents of (-)-menthide, which was preheated to the respective temperature in a copper-bath in the glove box. The reaction mixture was stirred for the given time, then an aliquot was taken and quenched by the addition of $CDCl_3$ (calculation of conversion via ^{1}H NMR spectroscopy). The reaction was quenched by addition of methanol. The polymer was precipitated in methanol, the solvent was decanted off or the polymer was isolated via centrifugation and the polymer was dried under vacuum at 60 °C overnight. Absolute molar masses and molar mass distributions were measured via SEC in tetrahydrofuran with triple detection.

Kinetic Measurements of (-)-Menthide by Aliquot Method

After dissolving 74.7 μmol (1.0 eq.) of catalyst **1** in 1.5 mL of toluene, this solution was added to the respective equivalents of (-)-menthide. At regular intervals, aliquots were taken from the reaction solution which were quenched by addition of $CDCl_3$. For each aliquot, the conversion was determined via ^{1}H NMR spectroscopy, and molar mass and polydispersity of the polymer sample was determined by SEC analysis in chloroform.

Copolymerization Procedure

After dissolving the calculated amount of catalyst **1** or **4** (24.9 μmol) in toluene (0.5 ml) at room temperature, this solution was added to the respective equivalents of (-)-menthide pre-heated to 60 °C or 100 °C in a copper-bath in the glove box. The reaction mixture was stirred for a given time-interval (2 to 6.5 h). One aliquot (0.1 ml) was taken and quenched by the addition of 0.4 ml $CDCl_3$ (calculation of conversion of (-)-menthide via ^1H NMR spectroscopy), while the calculated amount of rac-BBL was added to the reaction solution and stirred overnight at the respective temperature. Before quenching, a second aliquot was taken and quenched with 0.5 ml $CDCl_3$ to calculate the conversion of BBL via ^1H NMR spectroscopy. The polymers were precipitated and quenched by addition of methanol. The desired block copolymers were purified through washing with methanol and drying of the polymer overnight in a vacuum oven at 60 °C. The polymer sample of the first aliquot (block A) was dried overnight, the absolute molar mass and polydispersity of this block was determined by SEC analysis with triple detection in tetrahydrofuran. The polydispersity of the block copolymer was determined by SEC analysis in chloroform relative to polystyrene. An ^1H NMR spectrum of the block copolymer in $CDCl_3$ was measured to determine the ratio of PHB/PM. The molar mass of the block copolymer was determined through the ratio of PM/PHB (A/B) and the molar mass of block A. Composition A/B was calculated via comparison of the methine signal of PHB with the methine proton of the *iso*-propyl group of PM (Figure 3, right and SI, S11 and S13).

Menthide-polymerization with diphenylchlorophosphate as terminating agent

15 mg catalyst **4** (0.010 mmol, 1eq.) and 34.6 mg (-)-menthide (0.20 mmol, 20 eq.) were weighted into a screw cap vial in a glovebox, dissolved in 0.6 mL anhydrous C_6D_6 and heated up to 60 °C. After stirring overnight, 5.4 mg diphenylchlorophosphate were added and the reaction mixture was stirred for 20 min at 60 °C. ^{31}P NMR spectroscopy of the crude reaction mixture was used to elucidate the chain end-group and the mechanism of the polymerization.

2) Characterization of monomers

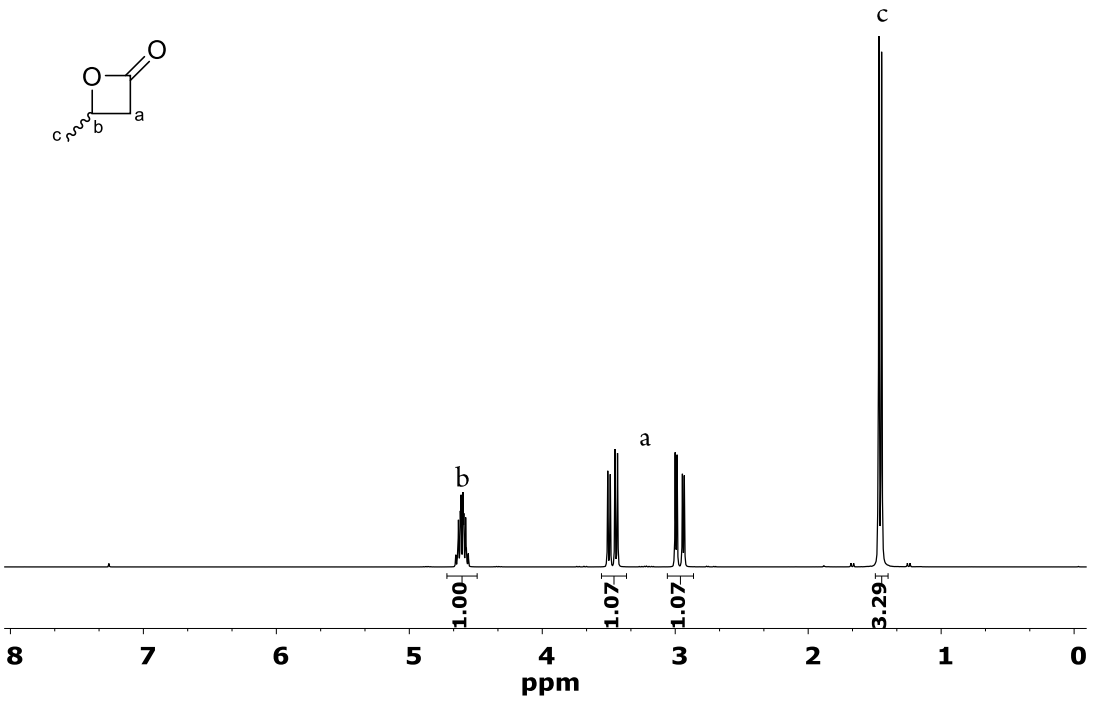

Figure S 1: ^{1}H-NMR spectrum of *rac*-BBL after distillation ($CDCl_3$, 300 MHz).

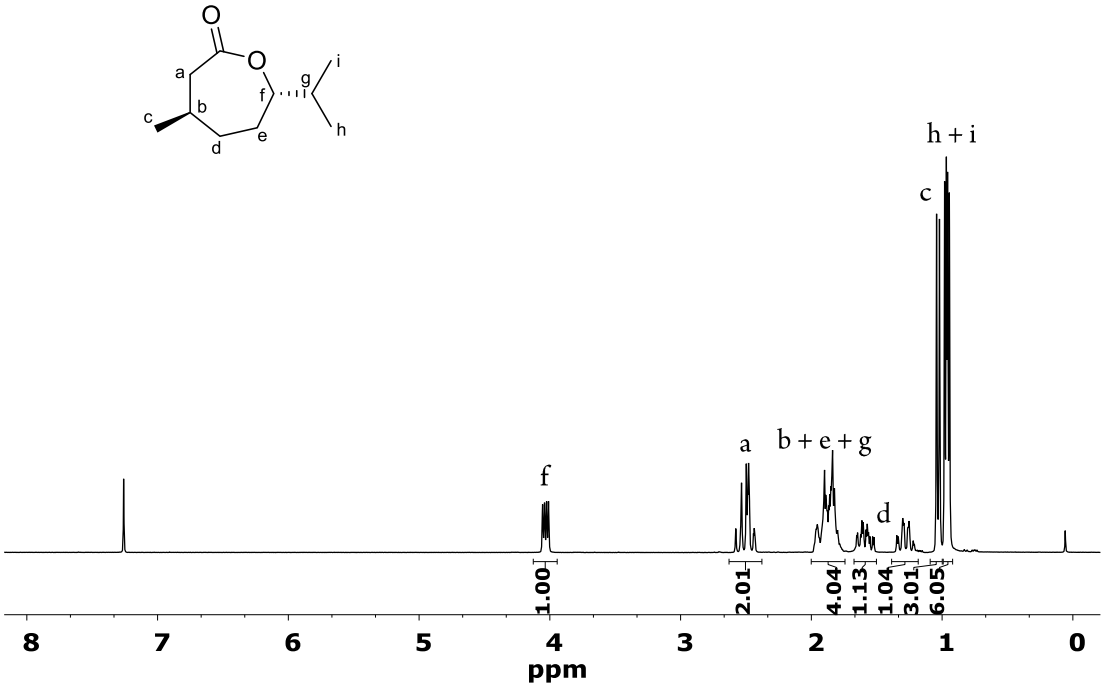

Figure S 2: ^{1}H-NMR spectrum of (-)-menthide after sublimation ($CDCl_3$, 300 MHz). Assignment according to Hillmyer and Tolman.[10]

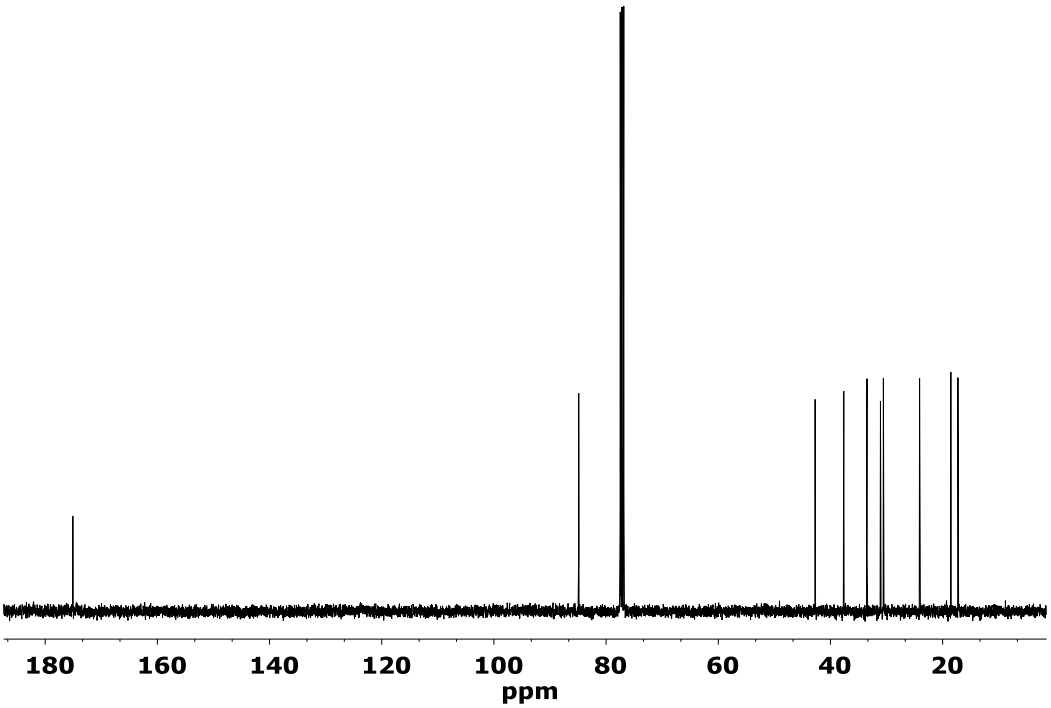

Figure S 3: ^{13}C-NMR spectrum of (-)-menthide (101 MHz, $CDCl_3$).

Elemental analysis of (-)-menthide:

calculated:	C 70.55	H 10.66
found:	C 70.52	H 10.78

GC-MS:

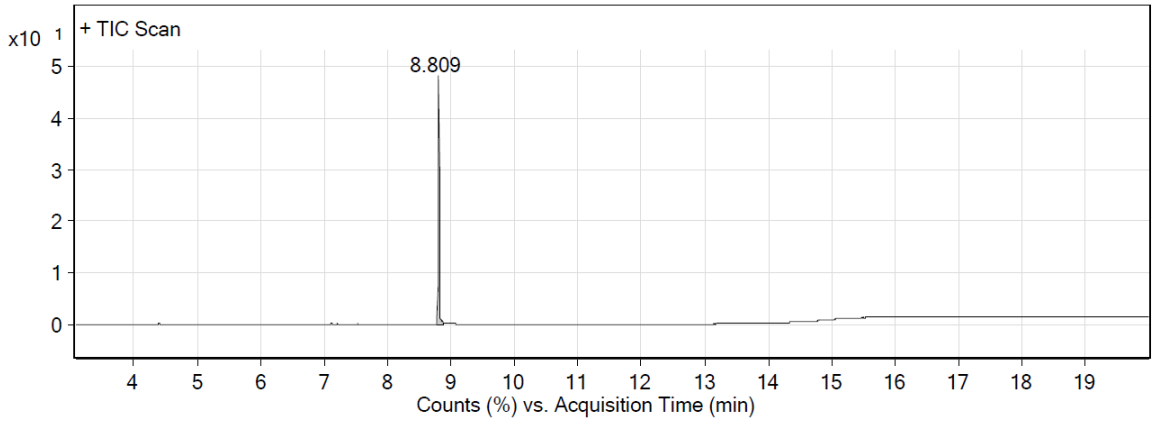

Integration Peak List

Peak	Start	RT	End	Height	Area	Area %
1	8.765	8.809	8.884	11761657.79	15740309.77	100

Qualitative Analysis Report

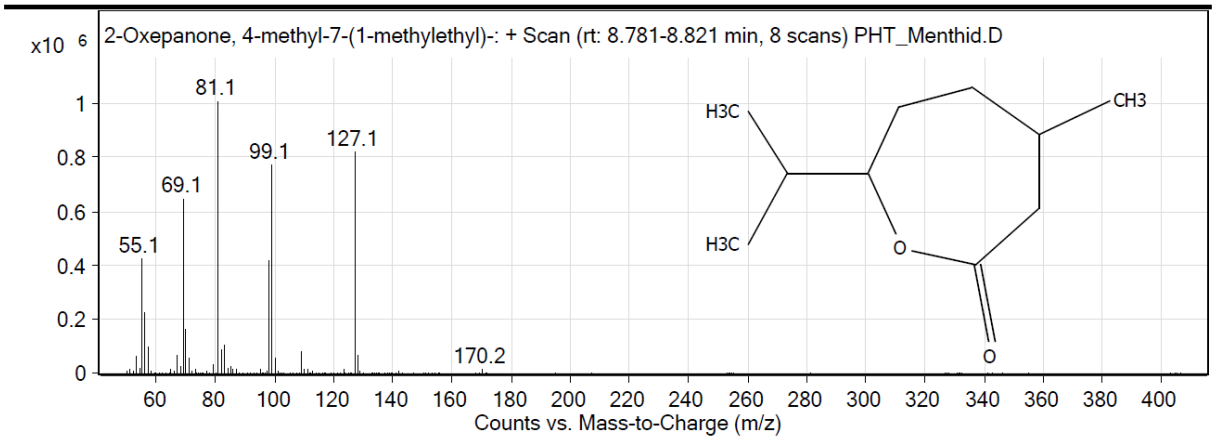

3) NMR spectra of polymers

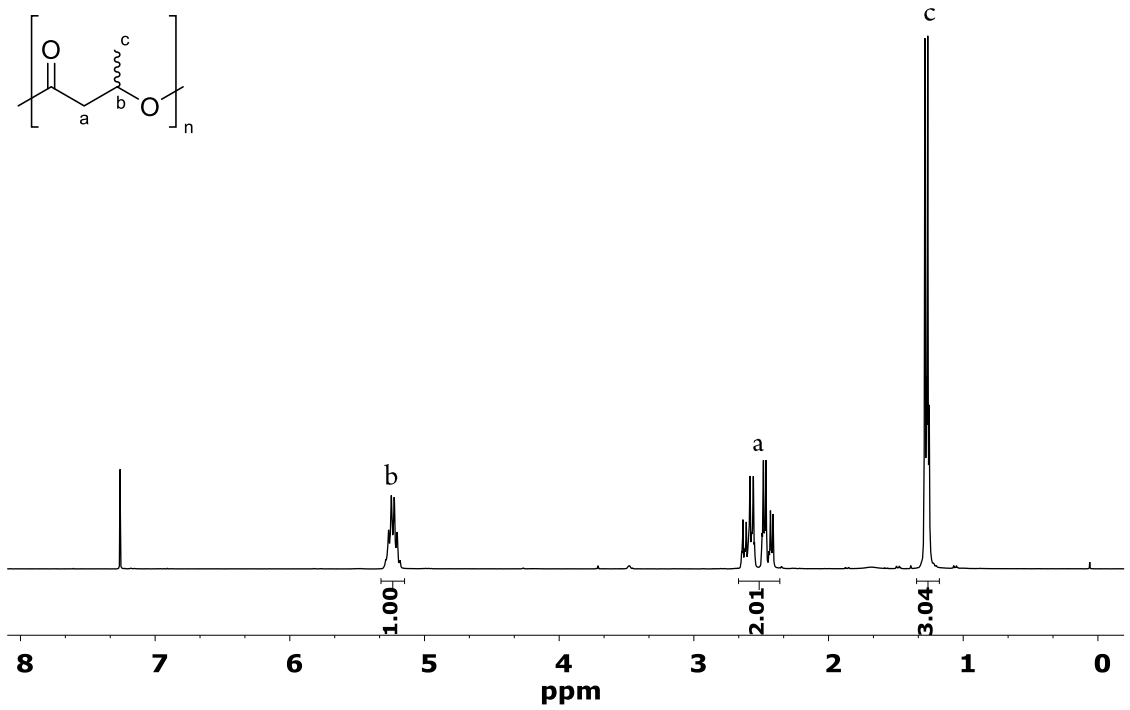

Figure S 4: ^{1}H-NMR spectrum of *syndio*-PHB (Table 2, Entry 9, 500 MHz, $CDCl_3$).

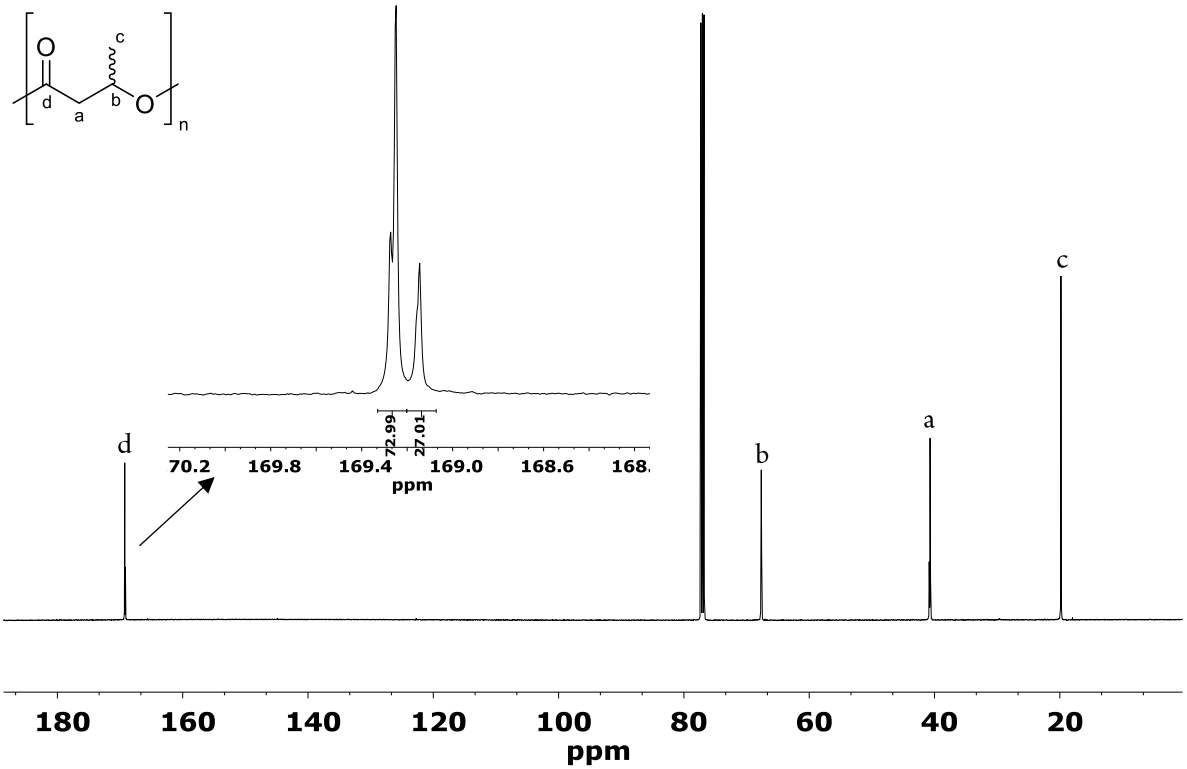

Figure S 5: ^{13}C-NMR spectrum of PHB with P_r = 0.73 (126 MHz, 1000 scans, $CDCl_3$, Table 2, Entry 9).

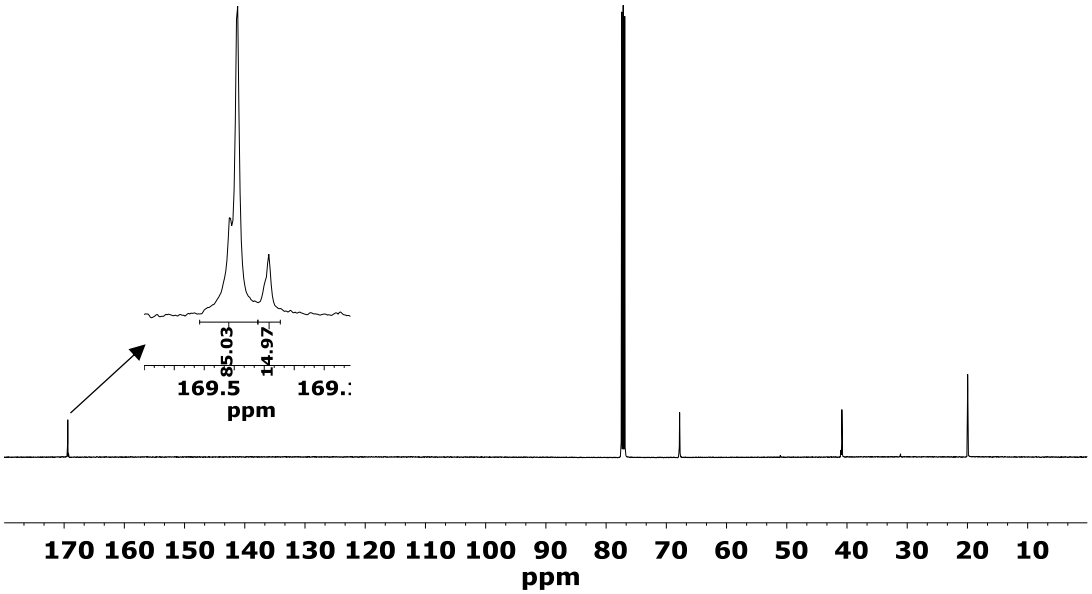

Figure S 6: ^{13}C-NMR spectrum of PHB with P_r = 0.85 (126 MHz, 1000 scans, $CDCl_3$, Table 1, Entry 4).

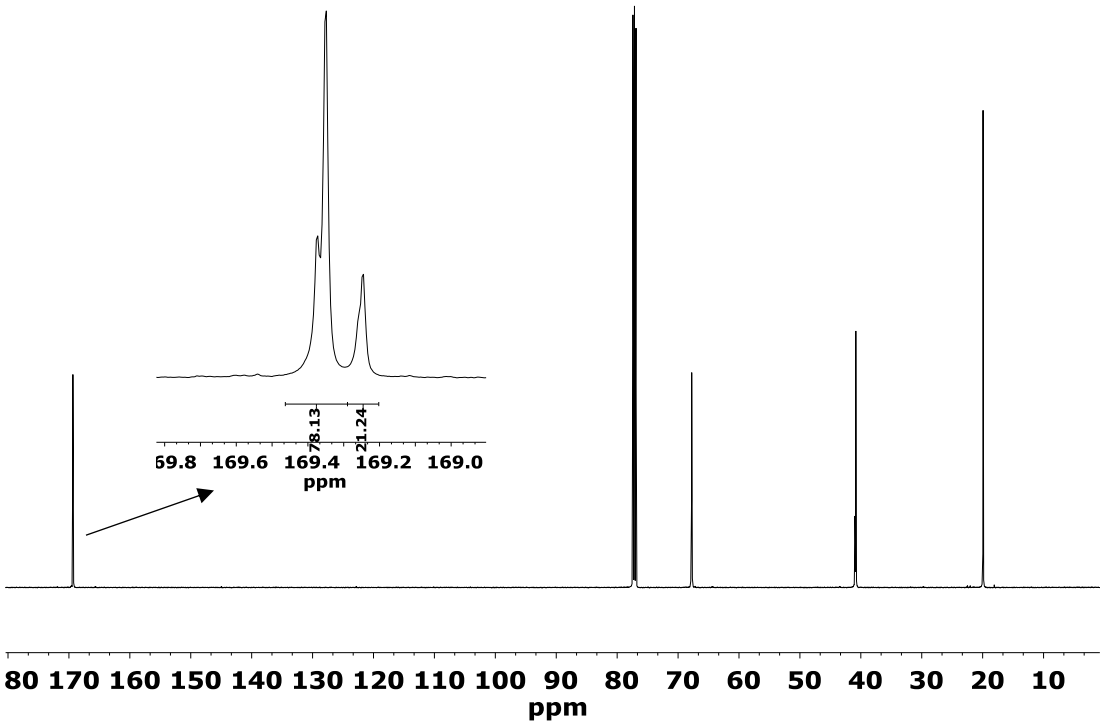

Figure S 7: ^{13}C-NMR spectrum of PHB with P_r = 0.78 (126 MHz, 1000 scans, $CDCl_3$, Table 2, Entry 7).

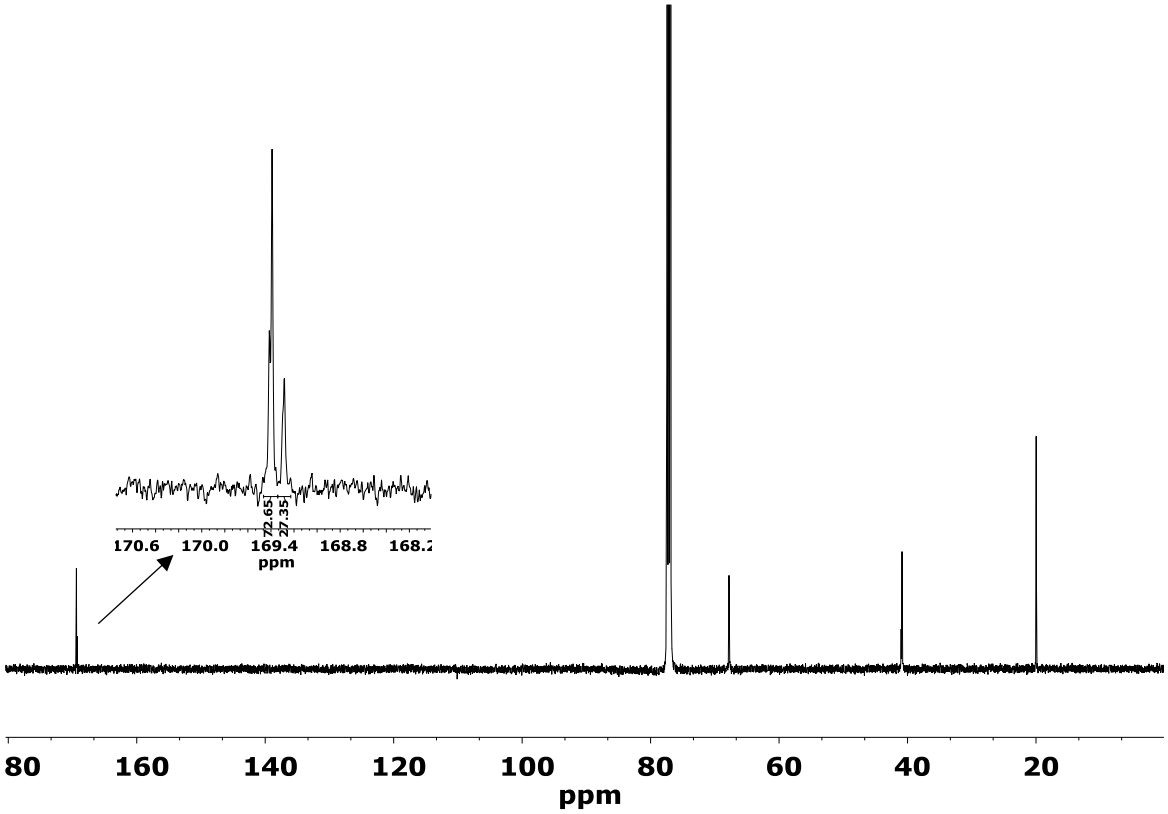

Figure S 8: ^{13}C-NMR spectrum of PHB with P_r = 0.73 (126 MHz, 1000 scans, $CDCl_3$, Table 2, Entry 2).

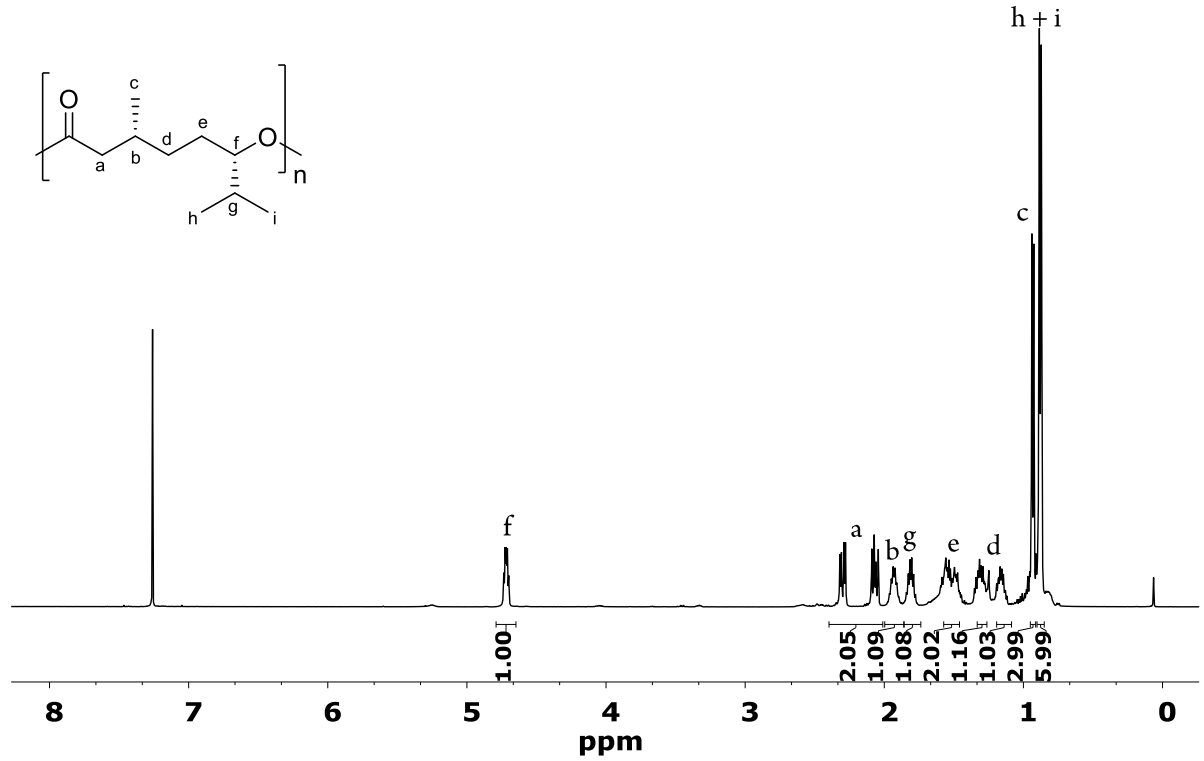

Figure S 9: ^{1}H-NMR spectrum of PM (Table 3, Entry 1, 500 MHz, $CDCl_3$). Assignment according to Hillmyer and Tolman.[10]

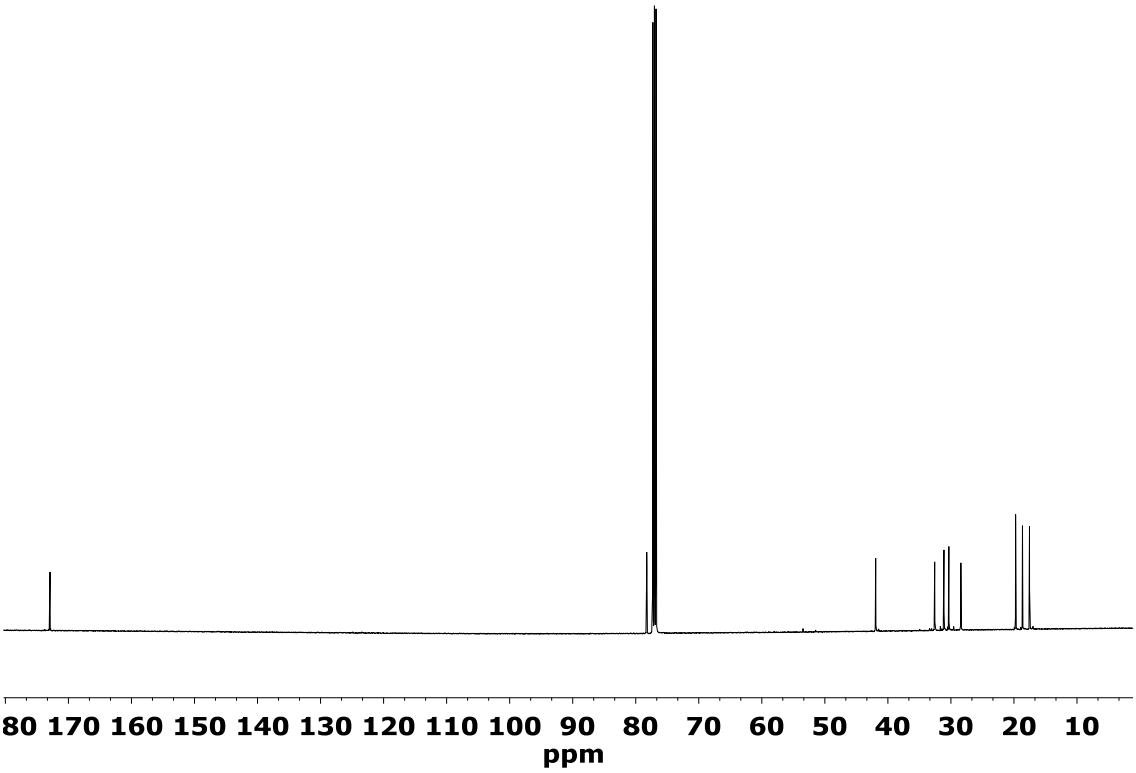

Figure S 10: ^{13}C-NMR spectrum of PM (126 MHz, 1000 scans, $CDCl_3$, Table 3, Entry 2).

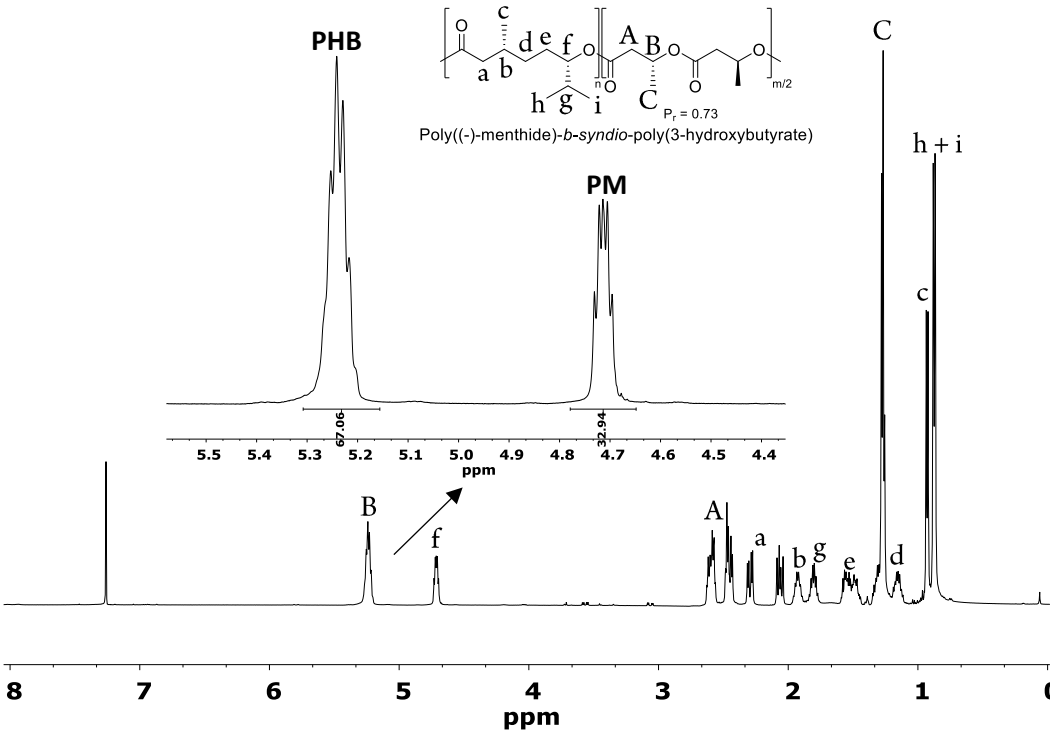

Figure S 11: ^{1}H-NMR spectrum of AB[1] (Table 4, Entry 1, 500 MHz, $CDCl_3$).

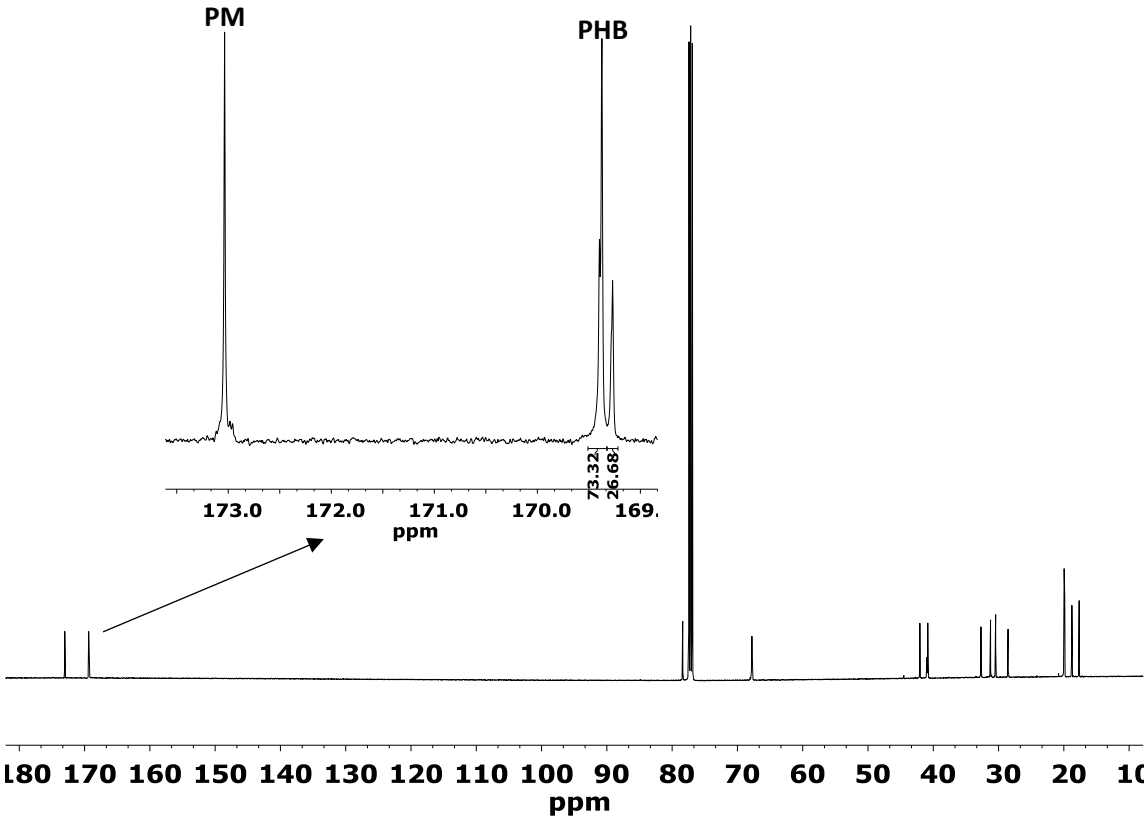

Figure S 12: ^{13}C-NMR spectrum of AB[1] (Table 4, Entry 1, 126 MHz, 1000 scans, $CDCl_3$).

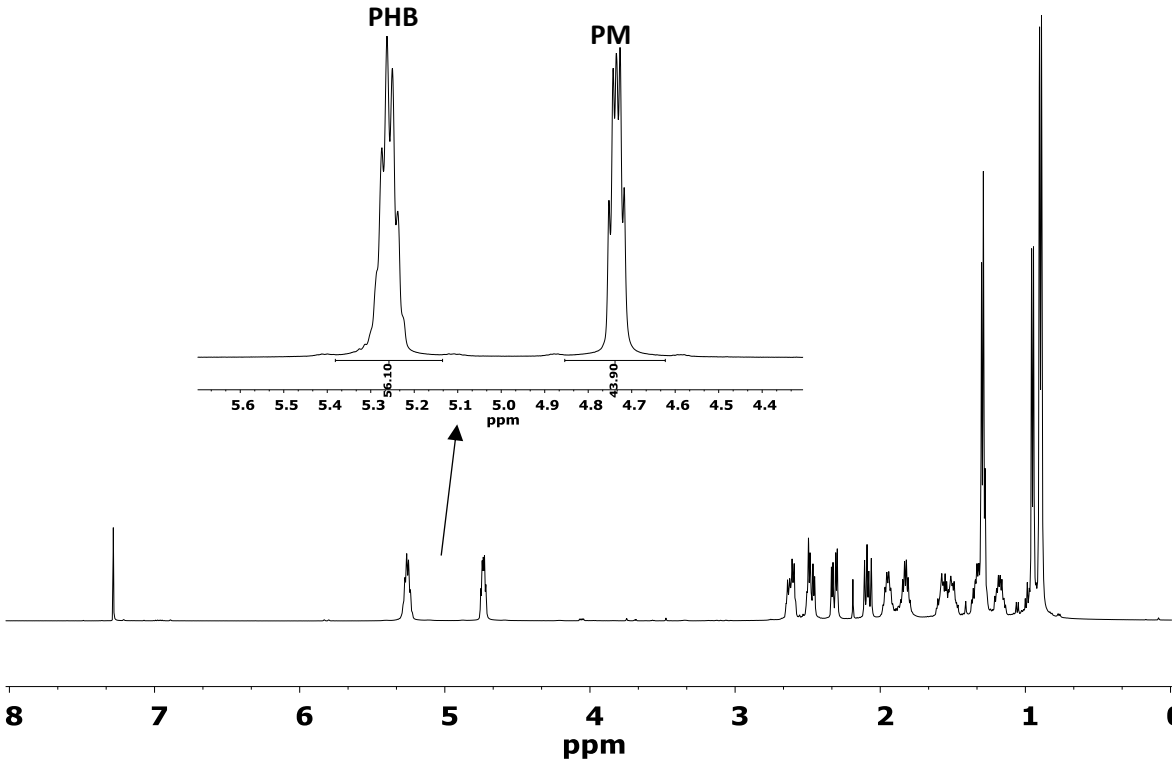

Figure S 13: ^{1}H-NMR spectrum of BAB[3] (Table 4, Entry 5, 500 MHz, $CDCl_3$).

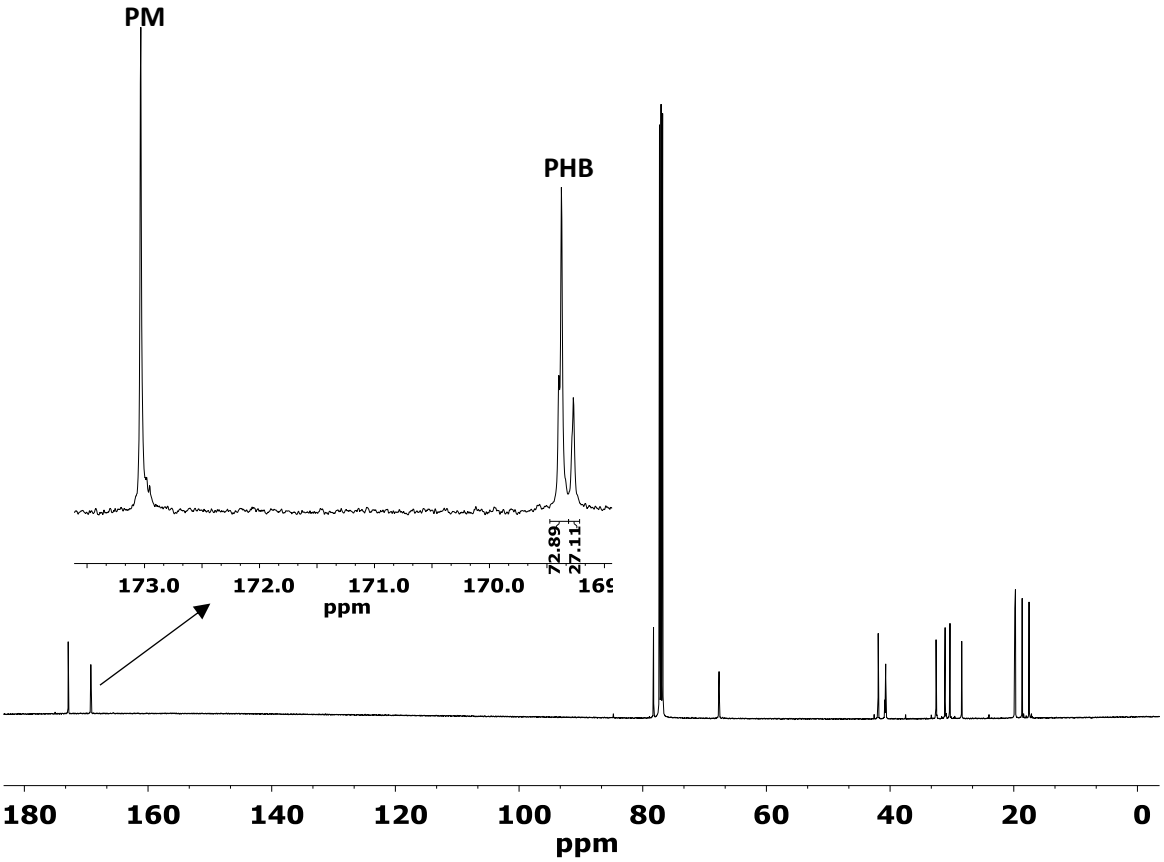

Figure S 14: ^{13}C-NMR spectrum of BAB^3 (Table 4, Entry 5, 126 MHz, 1000 scans, $CDCl_3$).

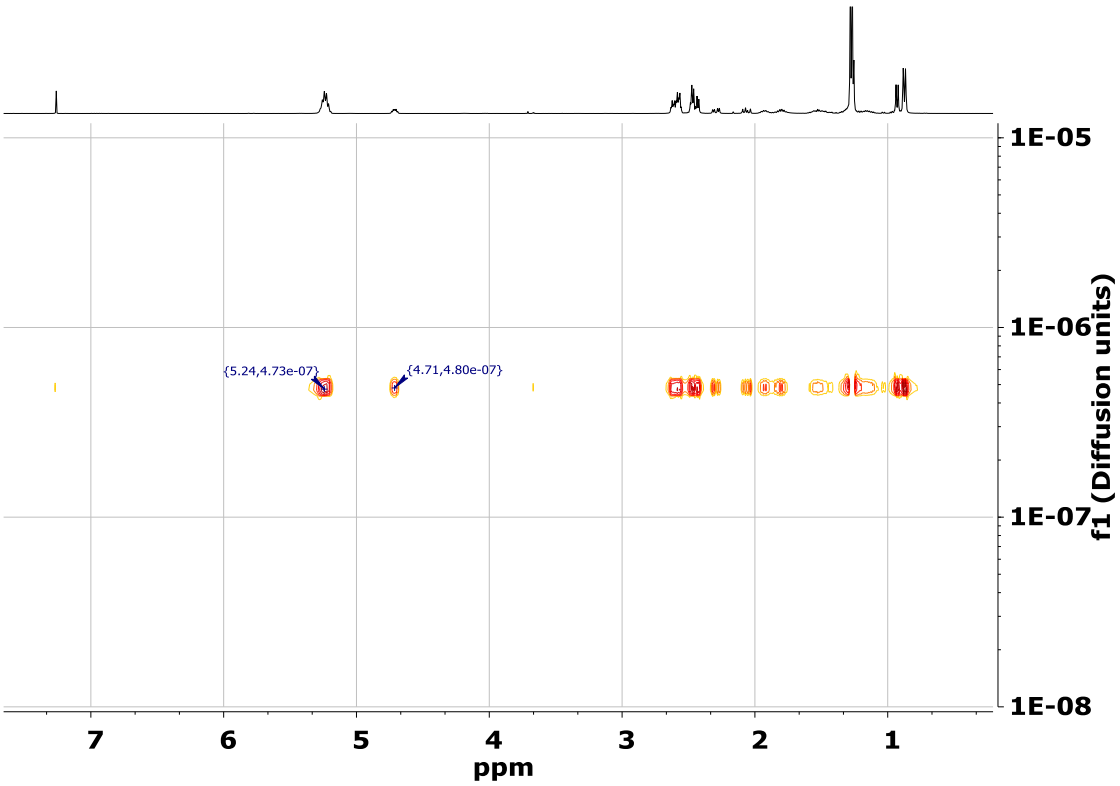

Figure S 15: DOSY-NMR of BAB[1] (Table 4, Entry 3, 400 MHz, 32 scans, $CDCl_3$, resolution factor: 1, repetitions: 1, points in diffusion dimension: 128).

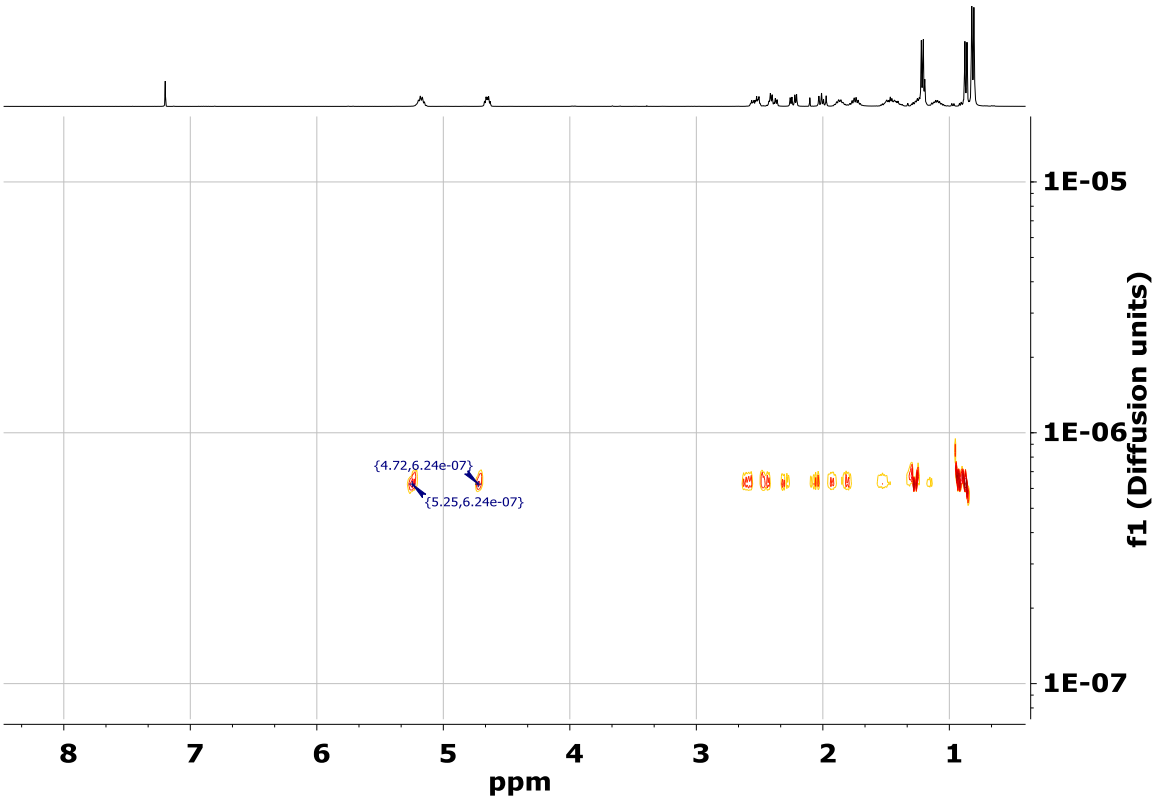

Figure S 16: DOSY-NMR of BAB[3] (Table 4, Entry 5, 400 MHz, 32 scans, $CDCl_3$, resolution factor: 1, repetitions: 1, points in diffusion dimension: 128).

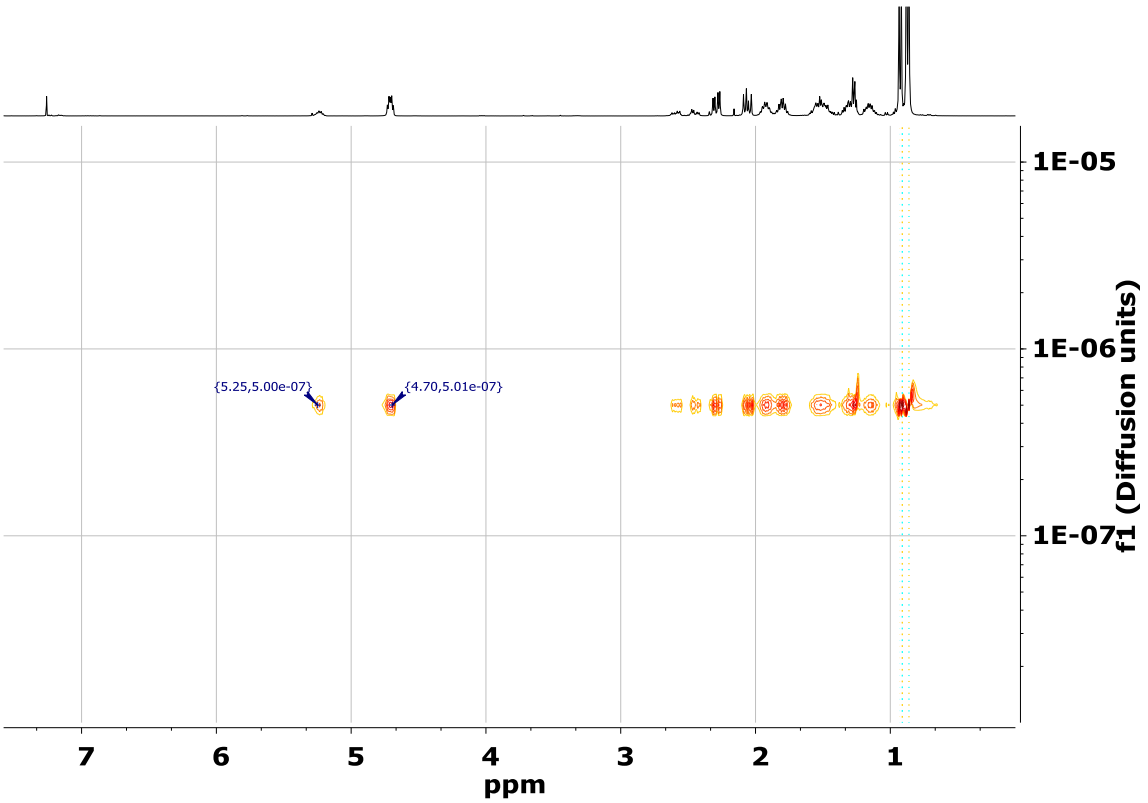

Figure S 17: DOSY-NMR of BAB[4] (Table 4, Entry 6, 400 MHz, 32 scans, $CDCl_3$, resolution factor: 1, repetitions: 1, points in diffusion dimension: 128).

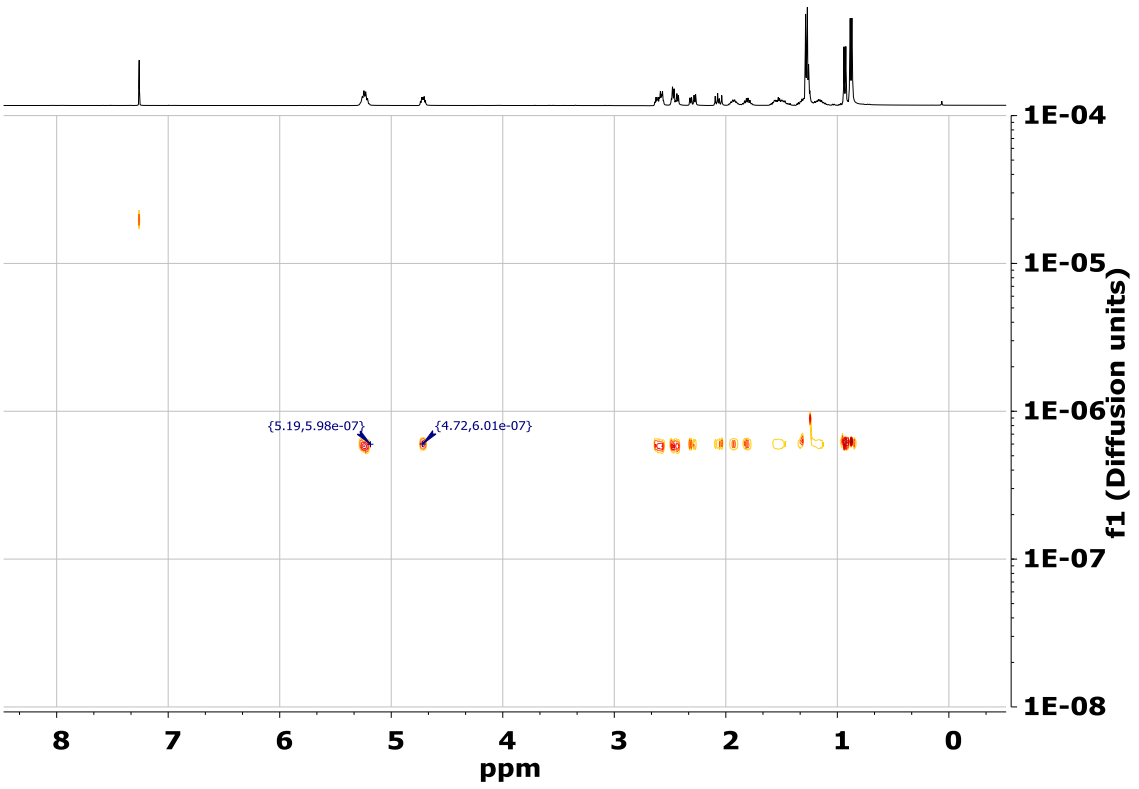

Figure S 18: DOSY-NMR of AB[1] (Table 4, Entry 1, 400 MHz, 32 scans, $CDCl_3$, resolution factor: 1, repetitions: 1, points in diffusion dimension: 128).

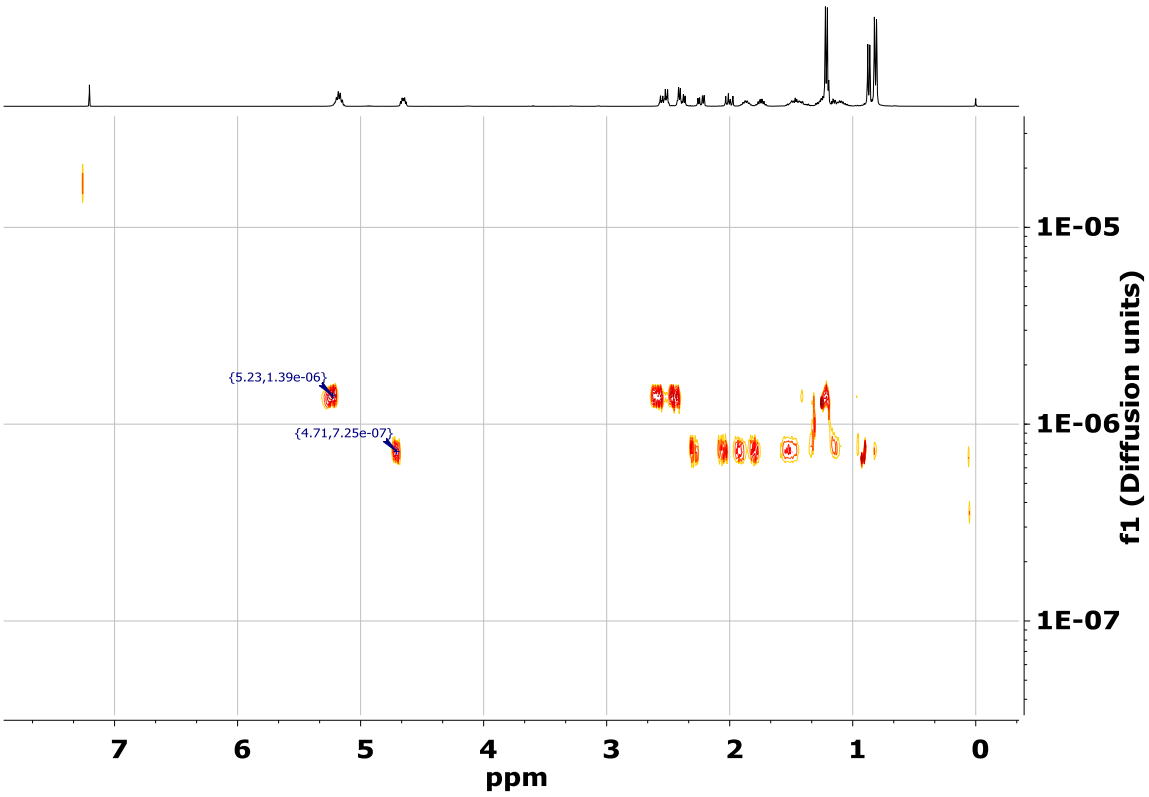

Figure S 19: DOSY-NMR of a blend from PM and PHB with the same composition (PM/PHB = 67:33; PM = 16800 g/mol) as AB[1] (400 MHz, 32 scans, $CDCl_3$, resolution factor: 1, repetitions: 1, points in diffusion dimension: 128).

4) ESI-MS analysis

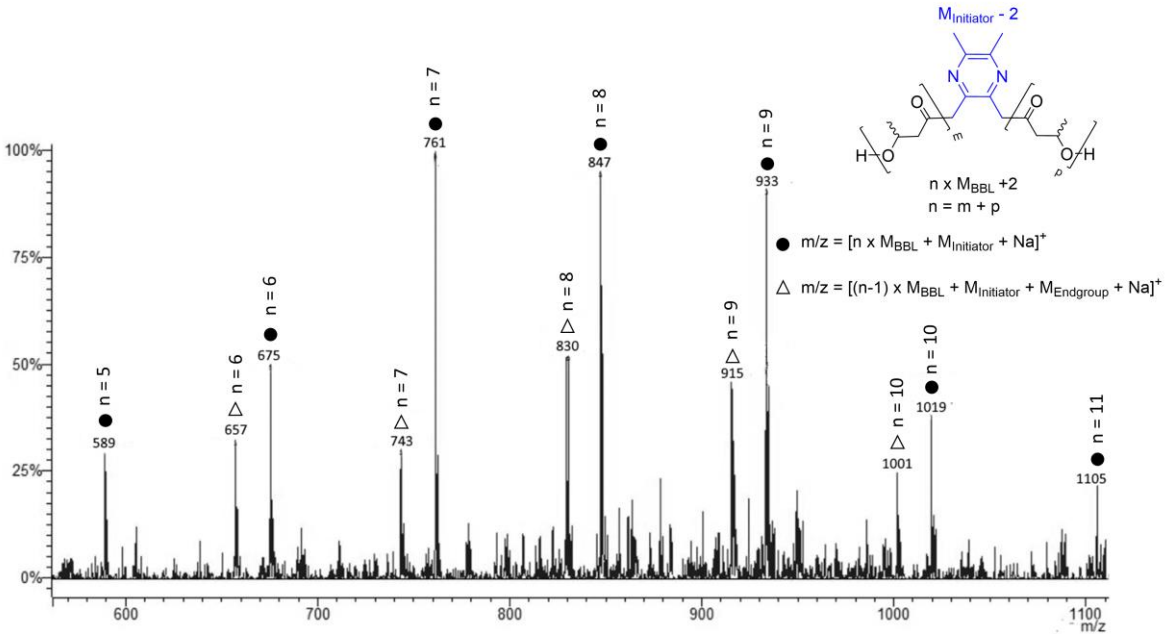

Figure S 20: End-group analysis by ESI-MS measured in acetonitrile with catalyst 4 and *rac*-BBL (7 µmol of catalyst, 93 µmol *rac*-BBL, 1 ml toluene, 20 °C).

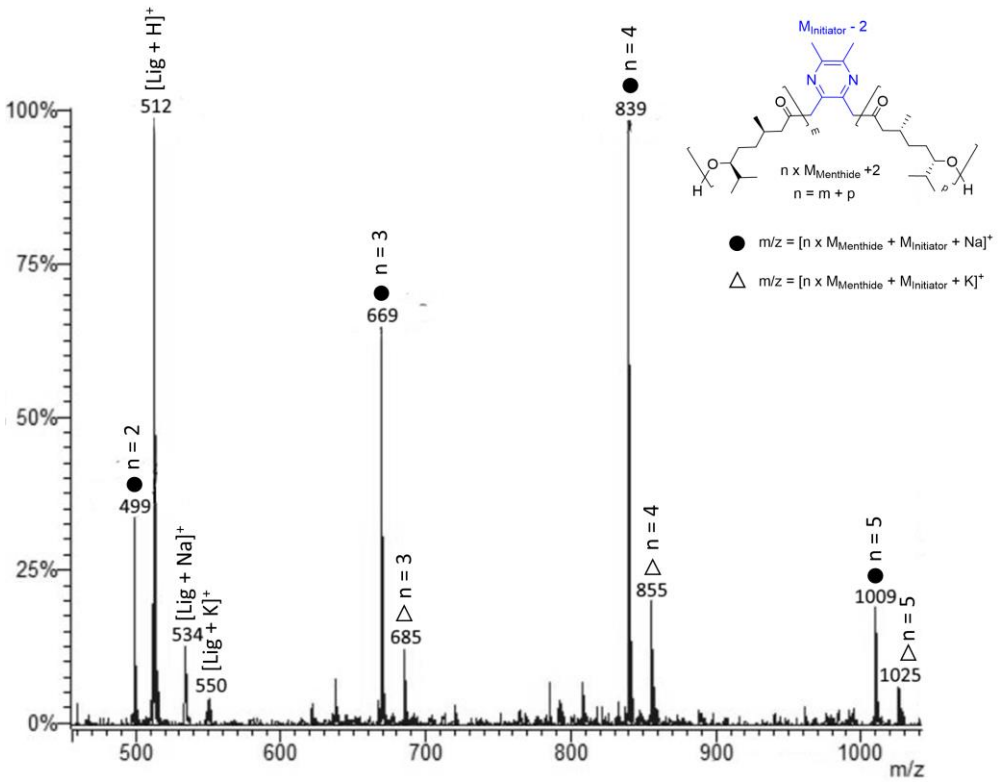

Figure S 21: End-group analysis by ESI-MS measured in acetonitrile with catalyst 4 and (-)-menthide (7 µmol of catalyst, 117 µmol (-)-menthide, 1 ml toluene, 20 °C).

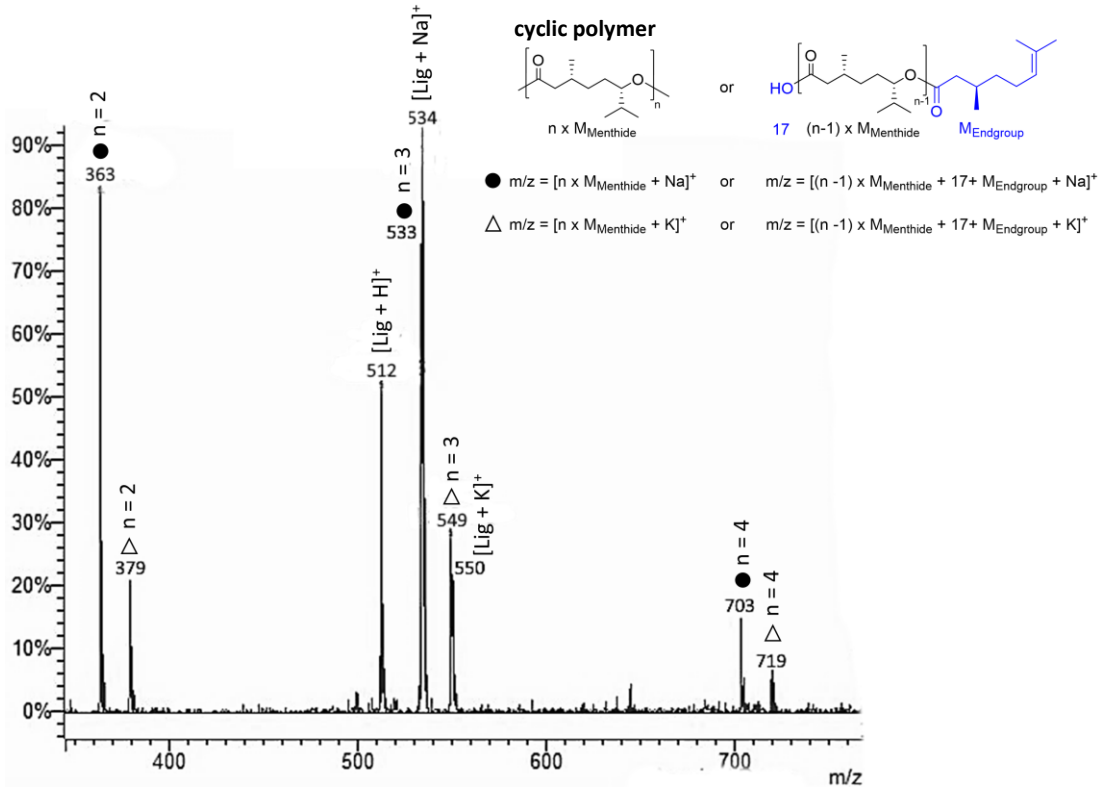

Figure S 22: End-group analysis by ESI-MS measured in acetonitrile with catalyst 1 and (-)-menthide (16 µmol of catalyst, 73 µmol (-)-menthide, 1 ml toluene, 20 °C).

5) SEC-traces

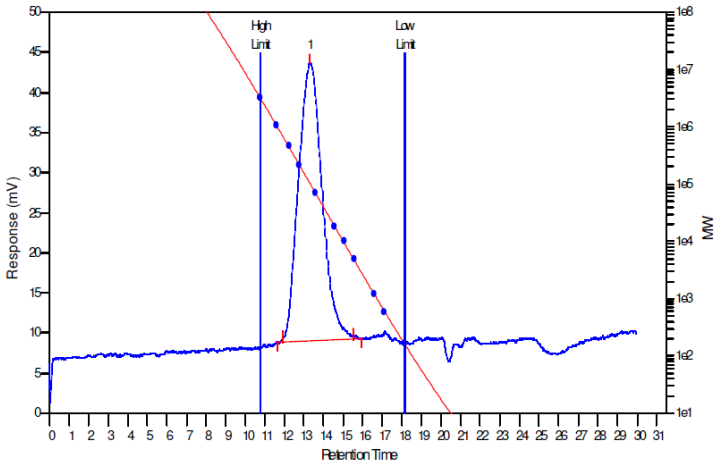

MW Averages

Peak No	Mp	Mn	Mw	Mz	Mz+1	Mv	PD
1	101292	66076	122933	192509	265667	113845	1.86048

Figure S 23: SEC trace in chloroform of PHB produced with catalyst 1 (Table 1, Entry 1).

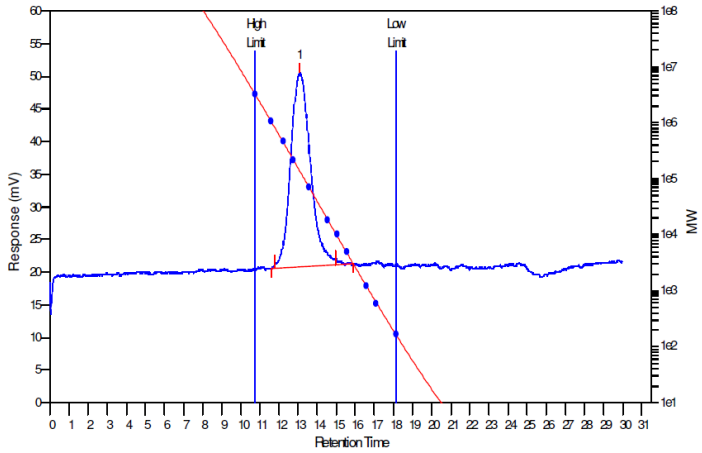

MW Averages

Peak No	Mp	Mn	Mw	Mz	Mz+1	Mv	PD
1	139420	91903	150558	220023	301920	141478	1.63823

Figure S 24: SEC trace in chloroform of PHB produced with catalyst 2 (Table 1, Entry 2).

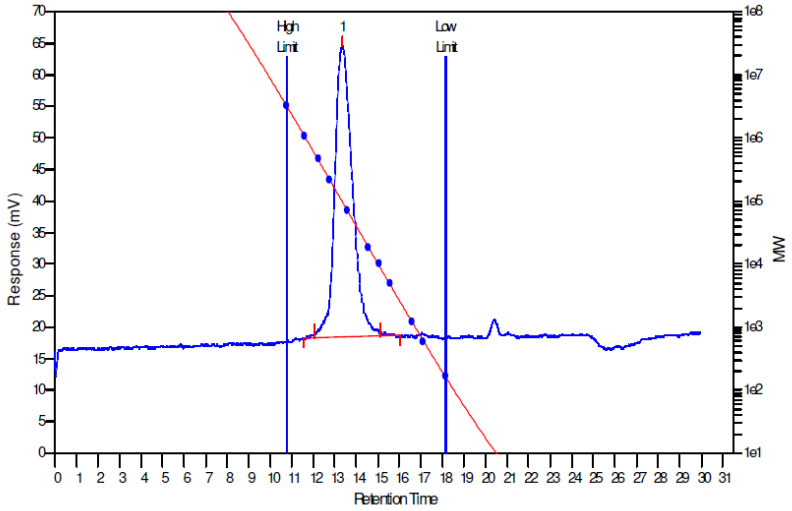

MW Averages

Peak No	Mp	Mn	Mw	Mz	Mz+1	Mv	PD
1	94587	68886	97668	134805	192075	93136	1.41782

Figure S 25: SEC trace in chloroform of PHB produced with catalyst 3 (Table 1, Entry 3).

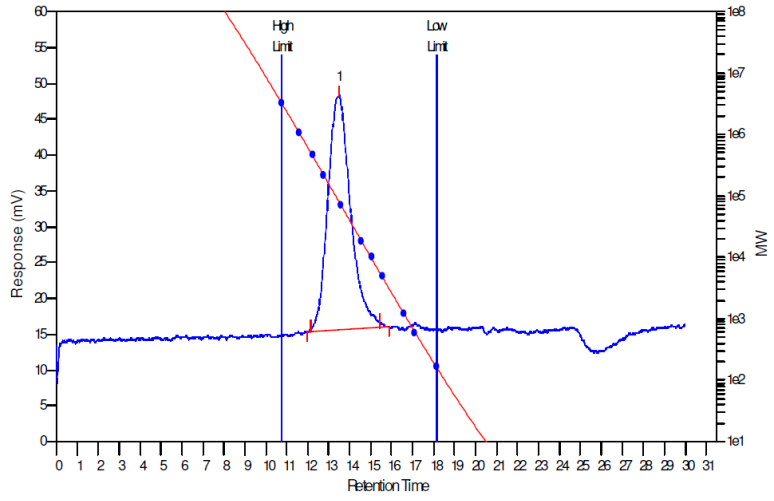

MW Averages

Peak No	Mp	Mn	Mw	Mz	Mz+1	Mv	PD
1	80614	52753	92064	137601	188215	86029	1.74519

Figure S 26: SEC trace in chloroform of PHB produced with catalyst 4 (Table 1, Entry 4).

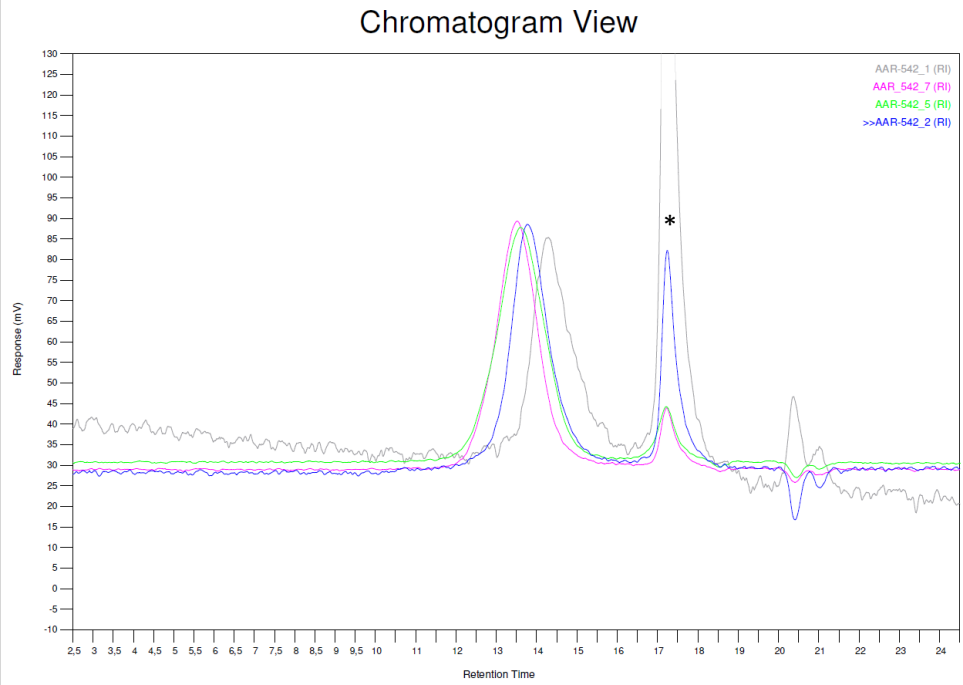

Figure S 27: Shift of molar masses during BBL-polymerization with catalyst 4 (Figure 3) measured via aliquot method (Aliquot 1 (grey), 2 (blue), 5 (green), and 7 (pink) are depicted). All samples are measured on a SEC in chloroform (* = residual menthide in aliquot samples).

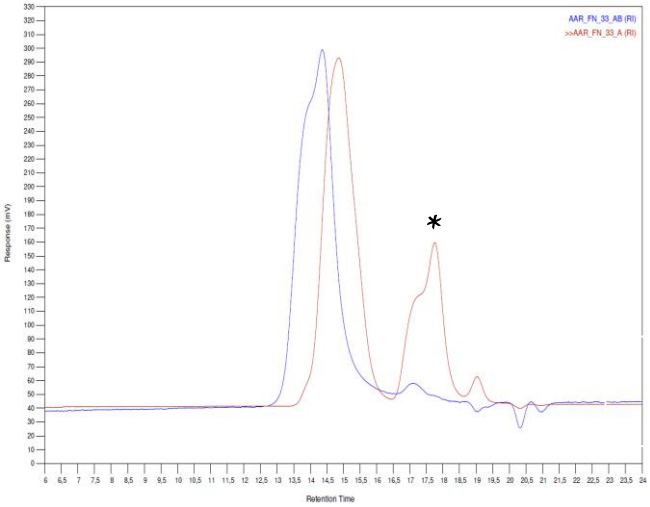

Figure S 28: Shift from Block A (red) to AB[1] (blue, Table 4, Entry 1). Both samples are measured on a SEC in chloroform (* = residual menthide in aliquot sample).

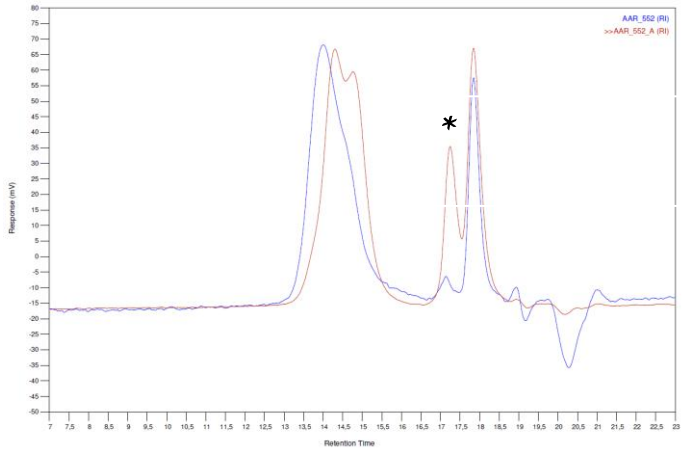

Figure S 29: Shift from Block A (red) to BAB[3] (blue, Table 4, Entry 5). Both samples are measured on a SEC in chloroform (* = residual menthide in aliquot sample).

Analysis Using Method: Triple

Results File: C:\Cirrus Workbooks\THF-2017-multi\30.05.2018-0002-Repeat (01).rst

Calculated dn/dc 0.067000; dn/dc used 0.067000

Ligt Scattering Results: Bulk IV 0.314186

LS 15° Mw: 33577 LS 90° Mw: 34209

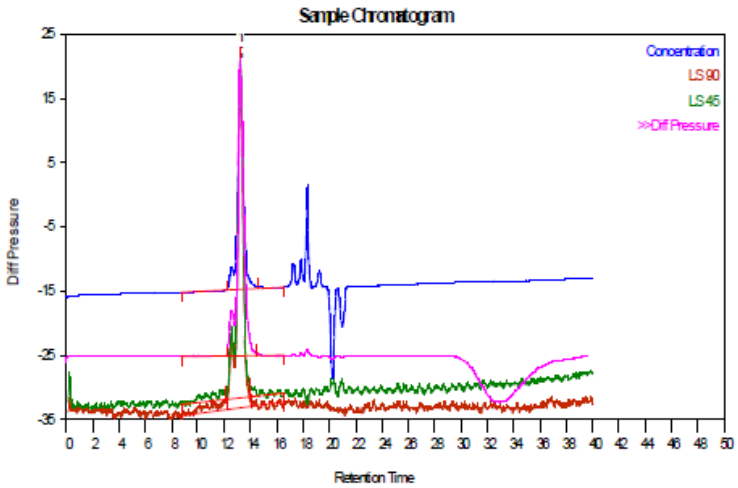

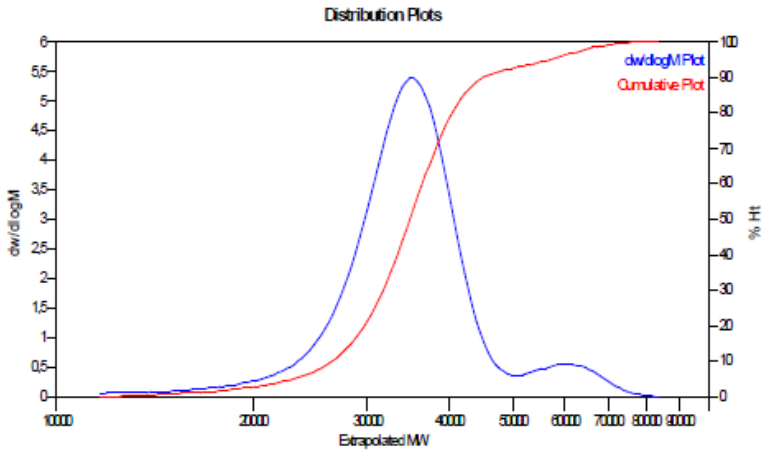

MW Averages

Peak No	Mp	Mn	Mw	Mz	Mz+1	Mv	PD
1	35300	33366	35635	38104	41028	34505	1.068

Figure S 30: SEC trace in tetrahydrofuran of PM produced with catalyst 1 (Table 3, Entry 1).

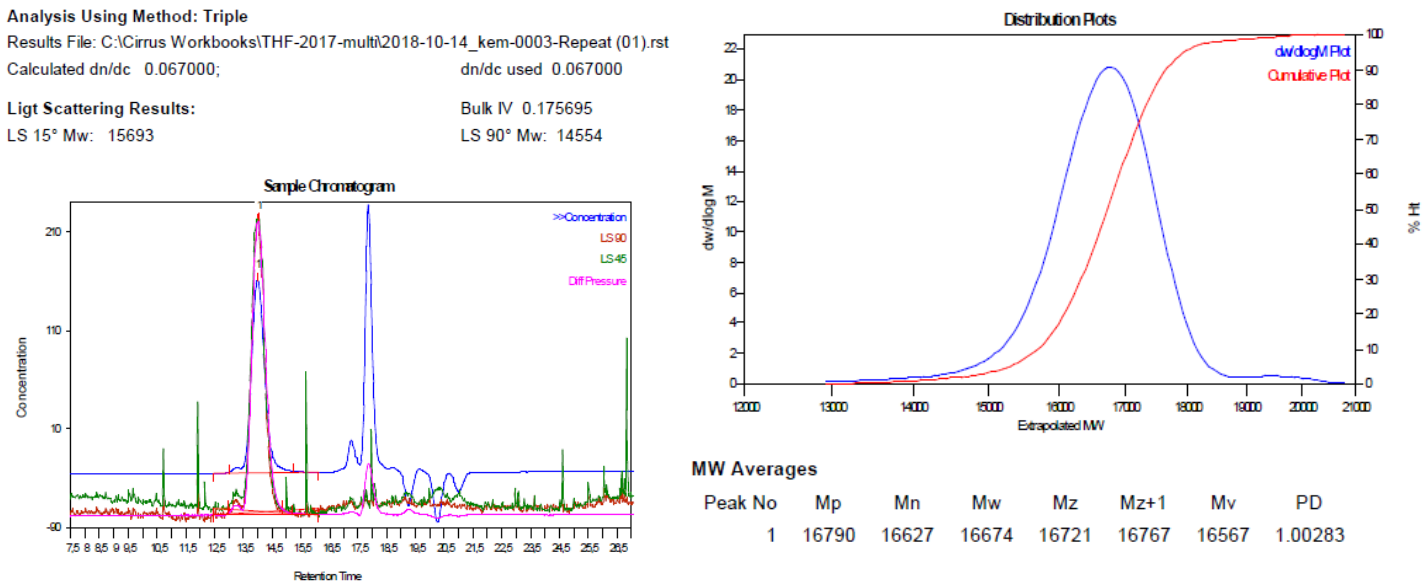

Figure S 31: SEC trace in tetrahydrofuran of PM produced with catalyst 2 (Table 3, Entry 5).

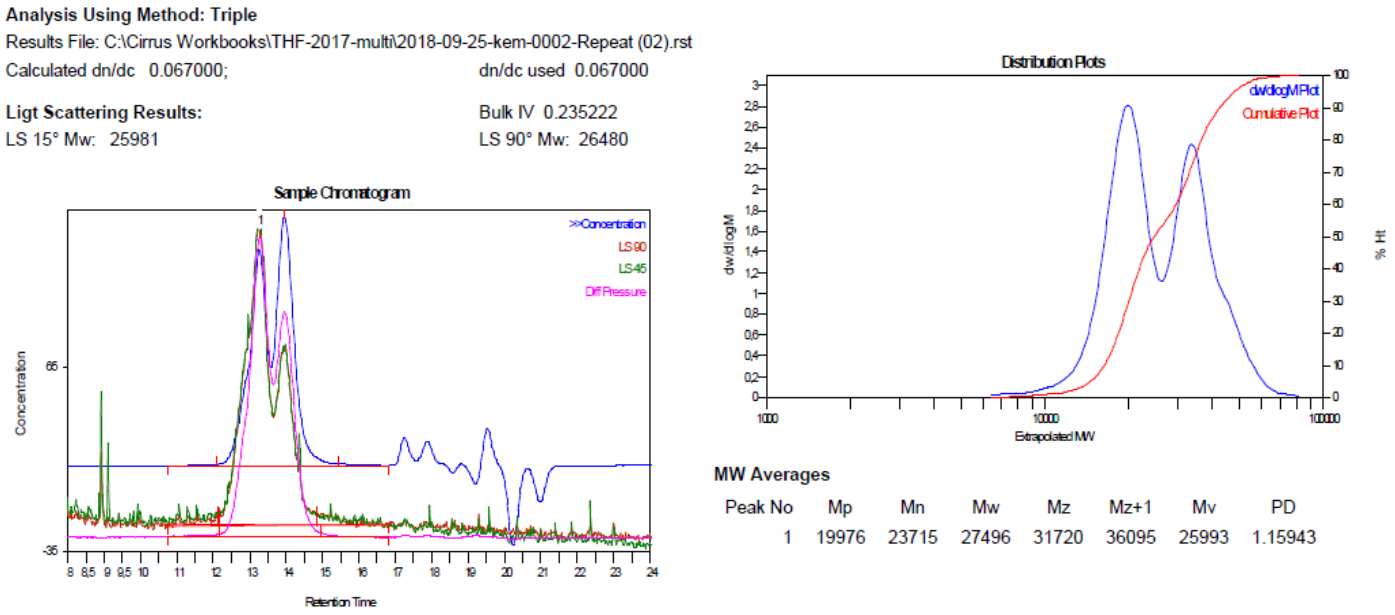

Figure S 32: SEC trace in tetrahydrofuran of PM produced with catalyst 4 (Table 3, Entry 6).

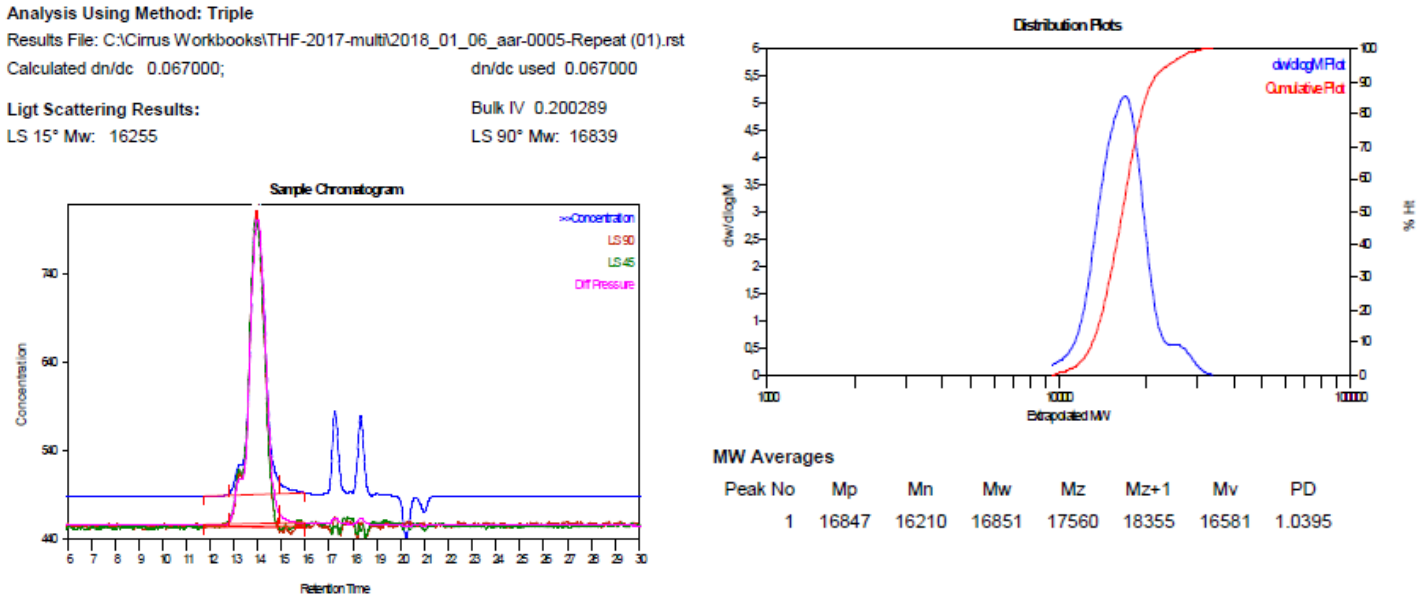

Figure S 33: SEC trace in tetrahydrofuran of Block A of AB[1] produced with catalyst 4 (Table 4, Entry 1).

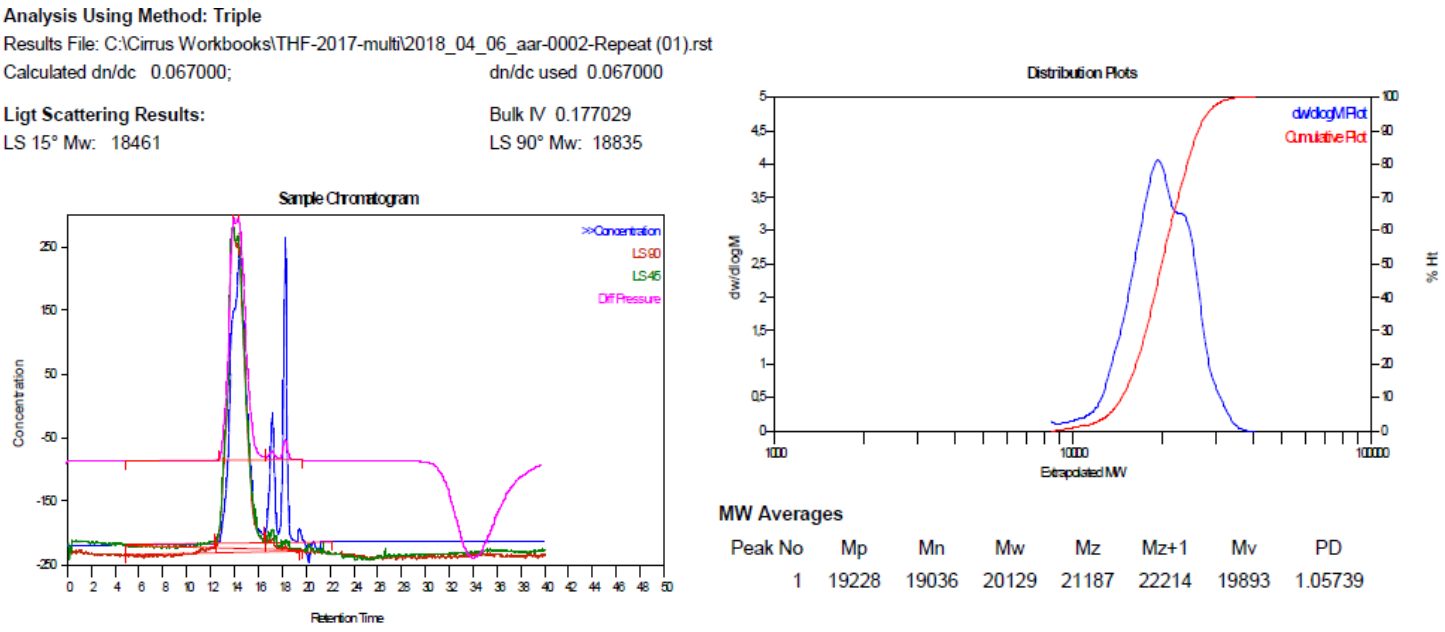

Figure S 34: SEC trace in tetrahydrofuran of Block A of BAB[2] produced with catalyst 4 (Table 4, Entry 4).

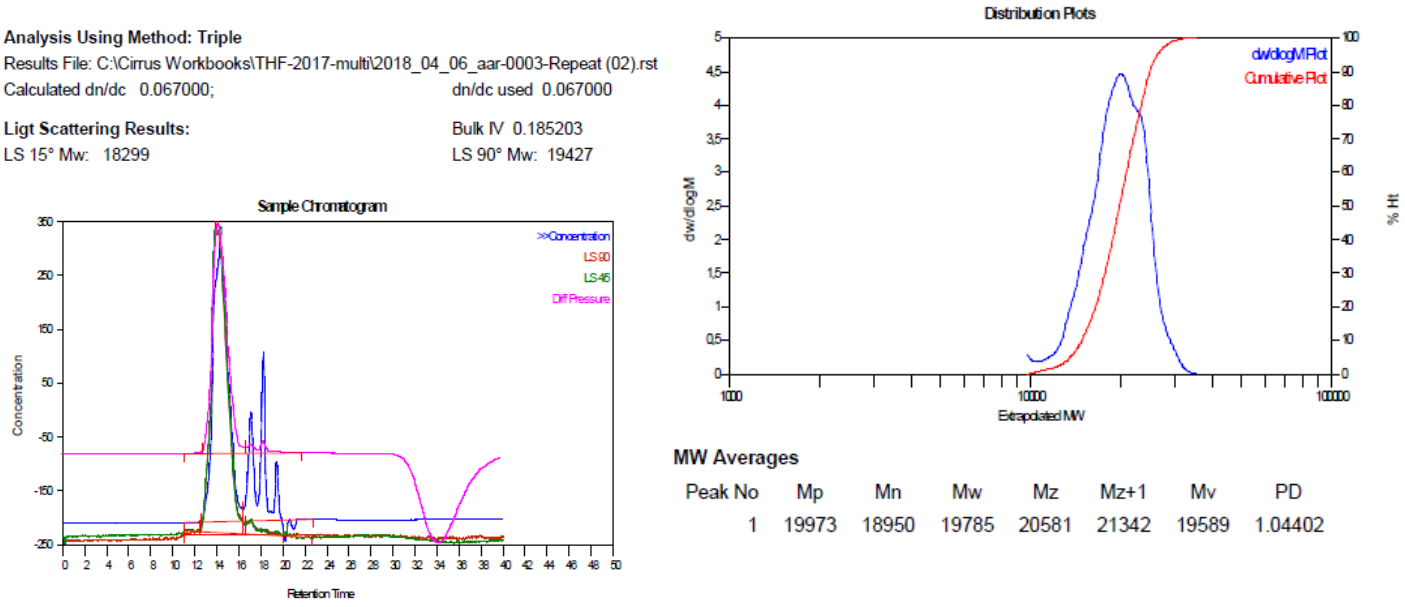

Figure S 35: SEC trace in tetrahydrofuran of Block A of BAB[4] produced with catalyst 4 (Table 4, Entry 6).

6) Kinetic measurements of *rac*-BBL with catalyst 4

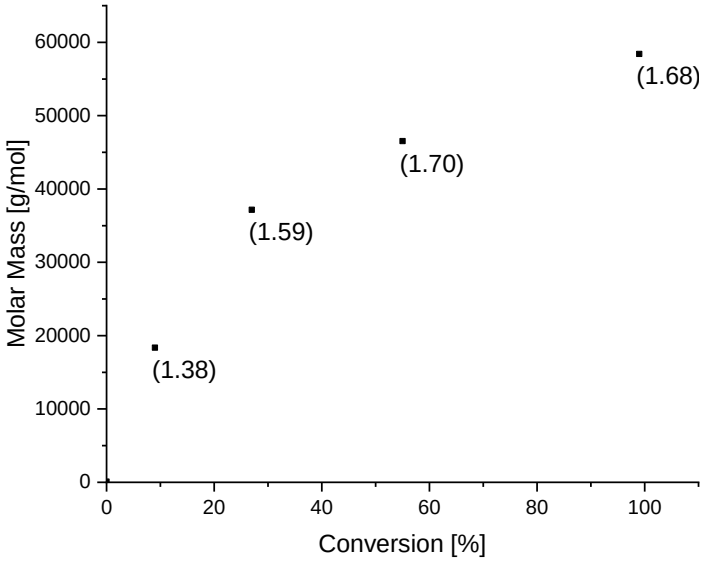

Figure S 36: Growth of the molar mass M_n [g/mol] (measured *via* SEC in chloroform) as a function of monomer conversion (determined via ^{1}H NMR spectroscopy) during BBL-polymerization with catalyst 4 (Đ in brackets).

7) Kinetic measurements of (-)-menthide with catalyst 1

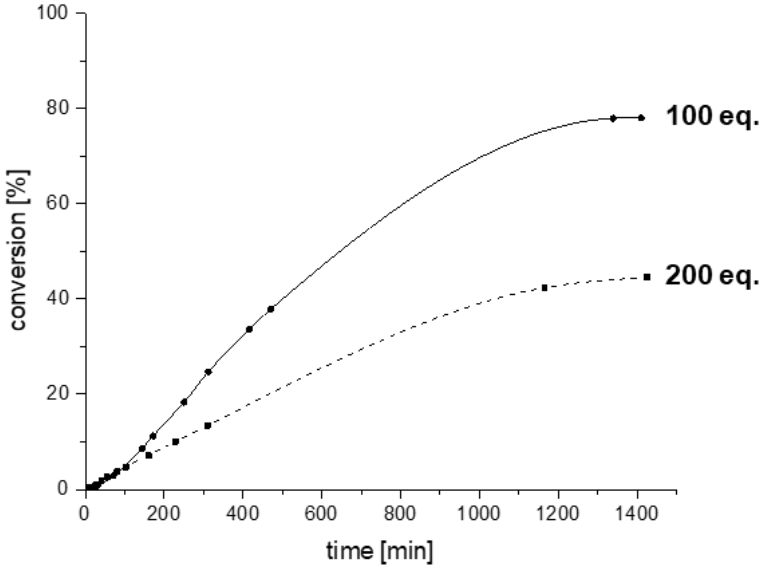

Figure S 37: Catalytic activity of catalyst 1 with 100 and 200 eq. of (-)-menthide ([cat.] = 74.7 µmol, toluene = 1.5 ml, T = 25 °C) measured *via* aliquot method. Conversion determined via ^{1}H-NMR spectroscopy.

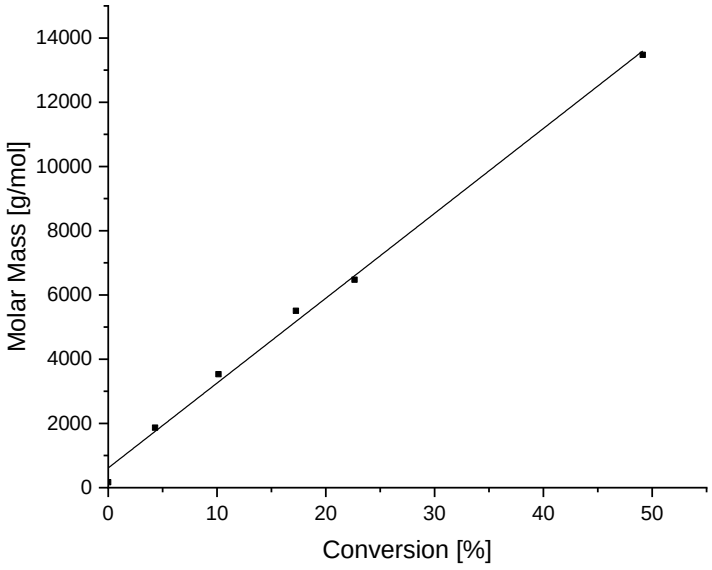

Figure S 38: Linear growth of the molar mass M_n [g/mol] (measured *via* SEC in chloroform) as a function of monomer conversion (determined via ^{1}H NMR spectroscopy) during (-)-menthide-polymerization (100 eq.) with catalyst 1.

8) Thermogravimetric analysis

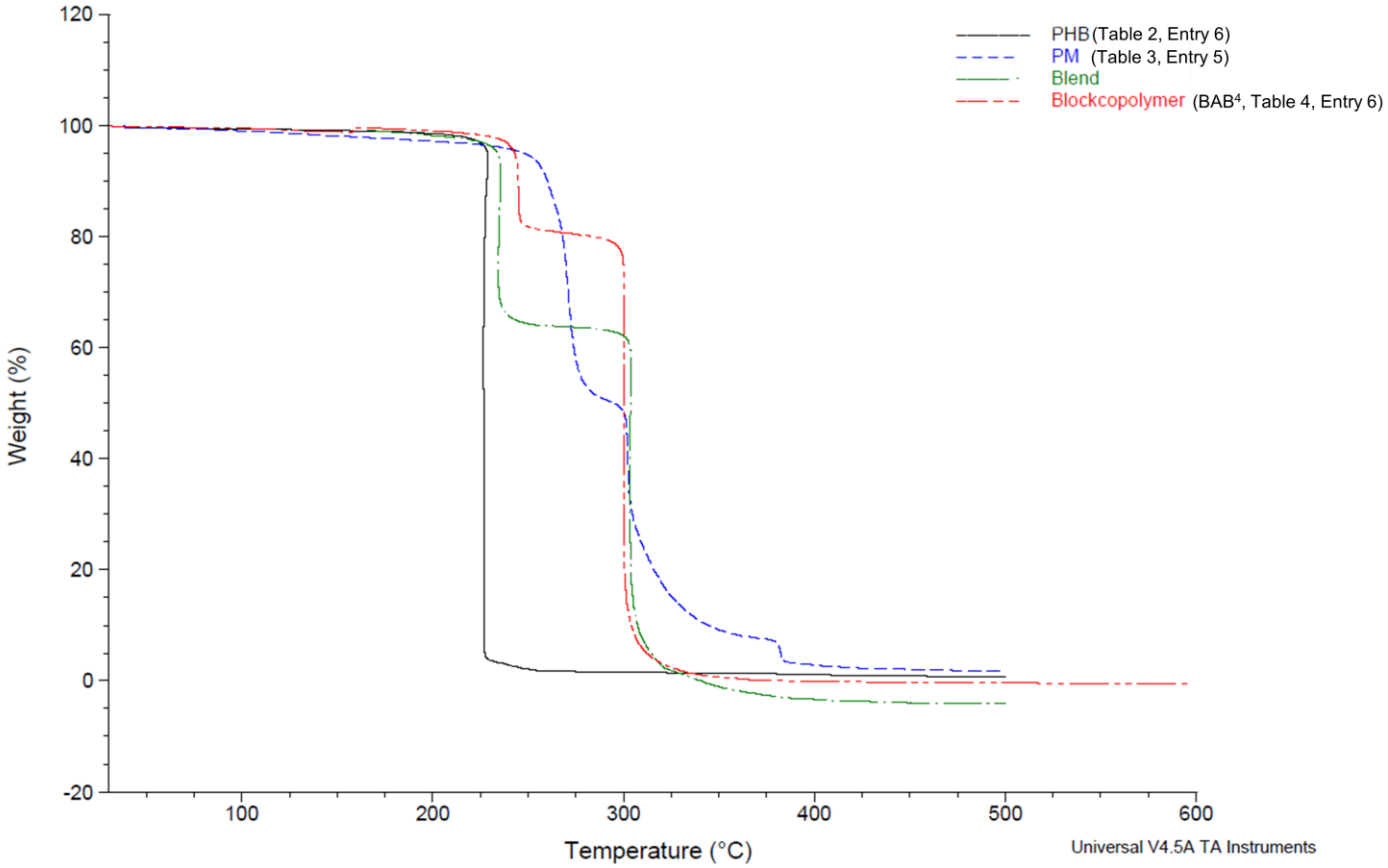

Figure S 39: High-resolution TGA of PHB (black), PM (blue), a blend of these two samples (green) and BAB^4 (red).

9) Differential scanning calorimetry

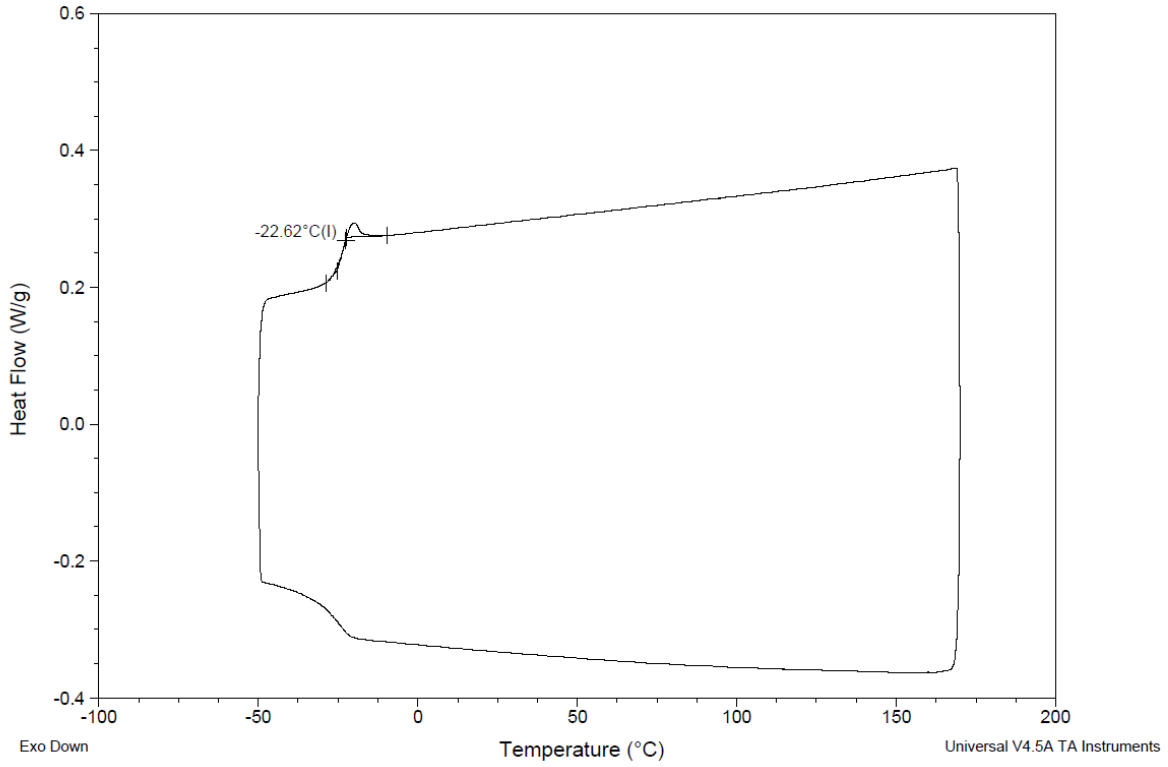

Figure S 40: DSC analysis of PM (Table 3, Entry 5).

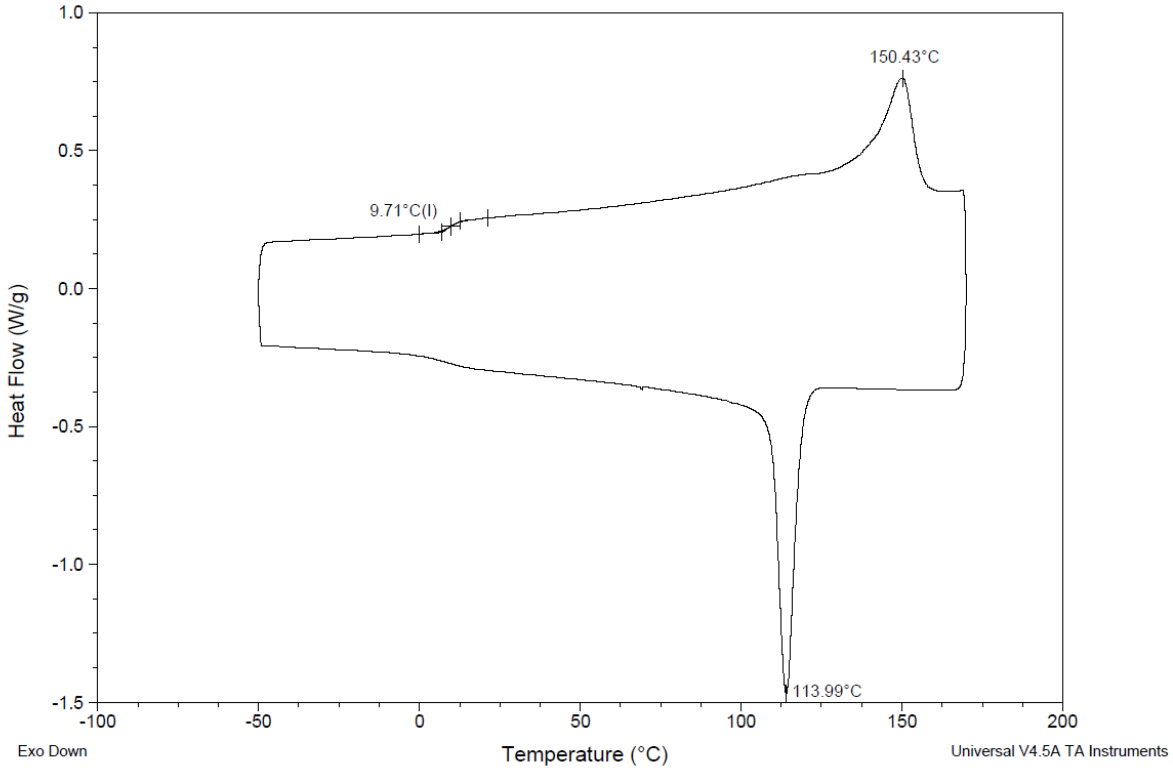

Figure S 41: DSC analysis of PHB (P_r = 0.85; Table 1, Entry 4).

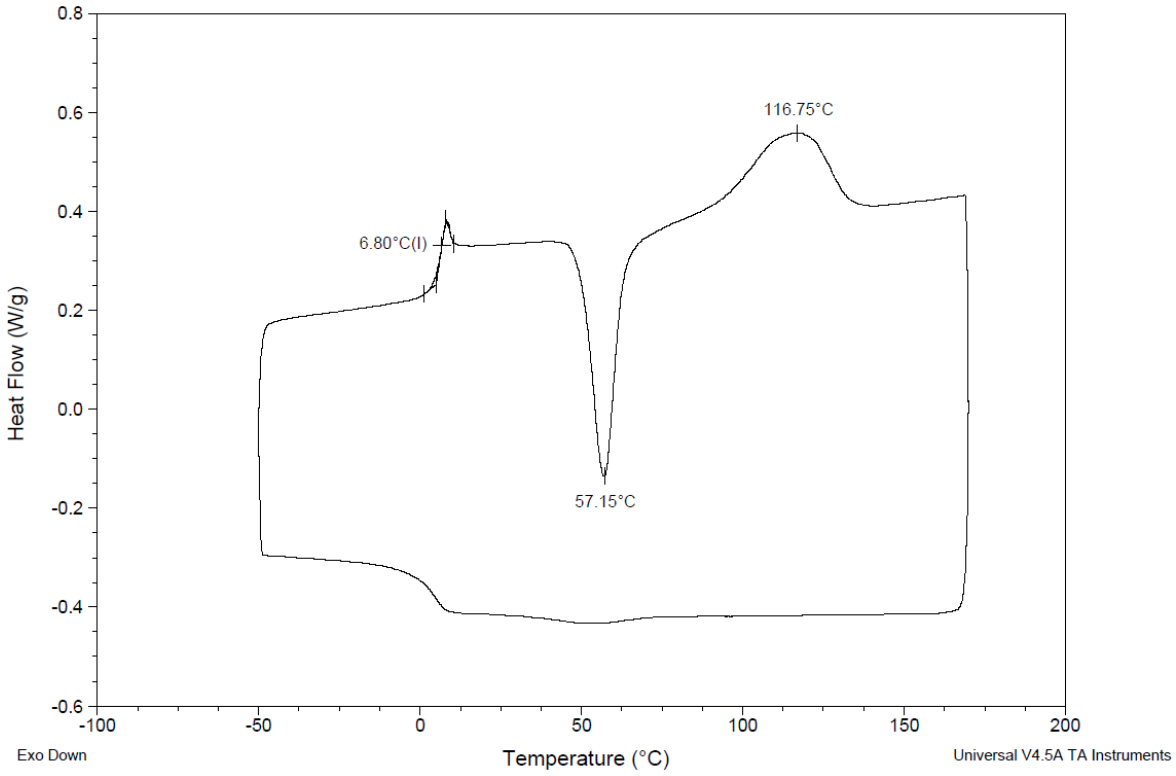

Figure S 42: DSC analysis of PHB (P_r = 0.74; Table 2, Entry 3).

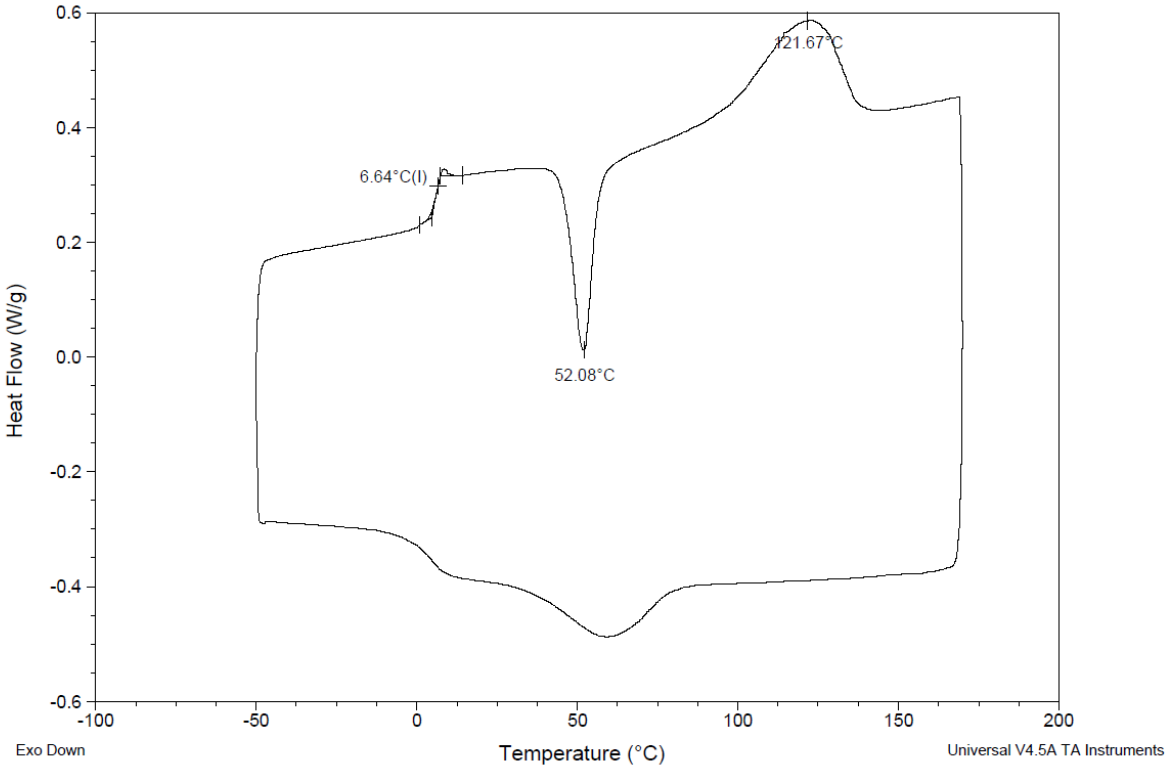

Figure S 43: DSC analysis of PHB (P_r = 0.73; Table 2, Entry 9).

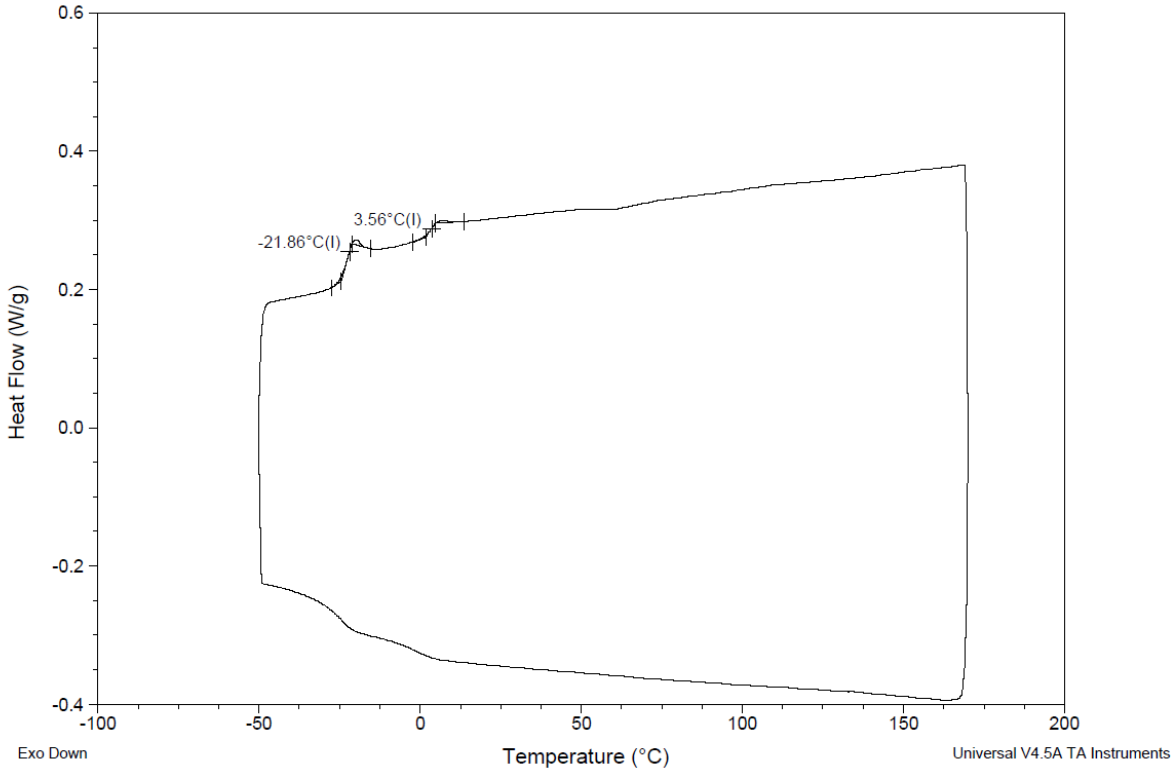

Figure S 44: DSC analysis of AB^2 (PM/PHB = 54/46; Table 4, Entry 2).

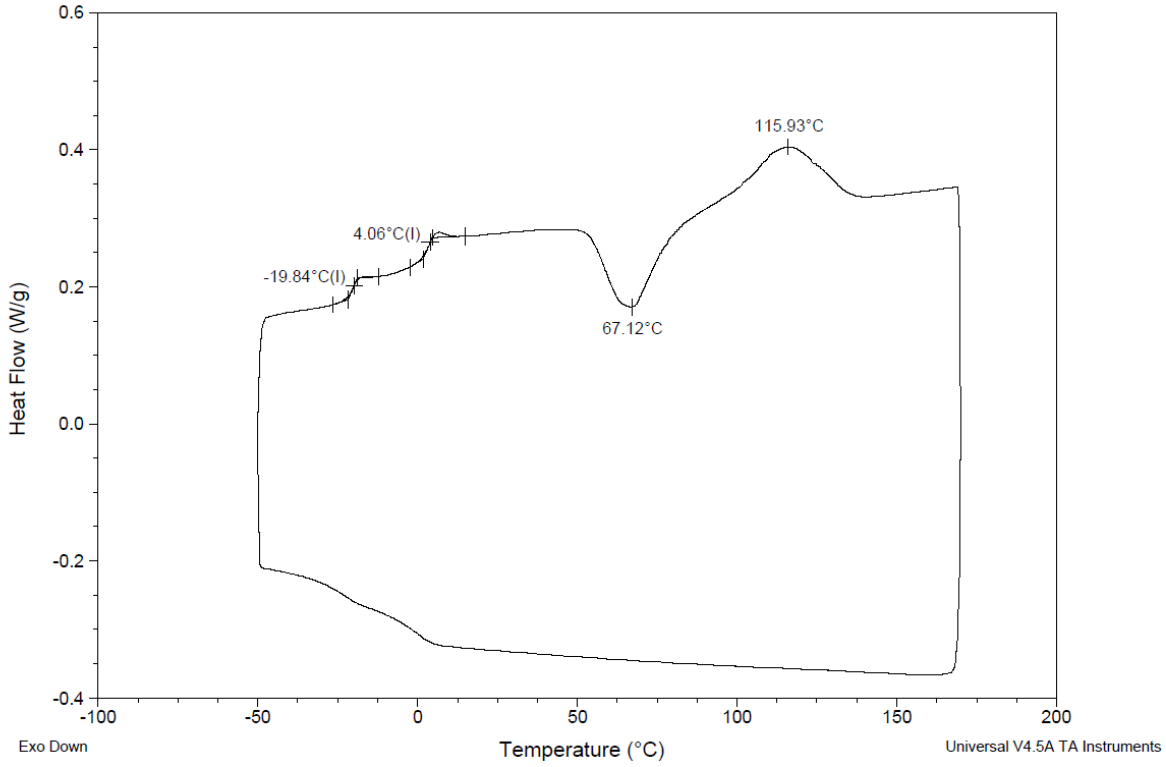

Figure S 45: DSC analysis of BAB^2 (PM/PHB = 30/70; Table 4, Entry 4).

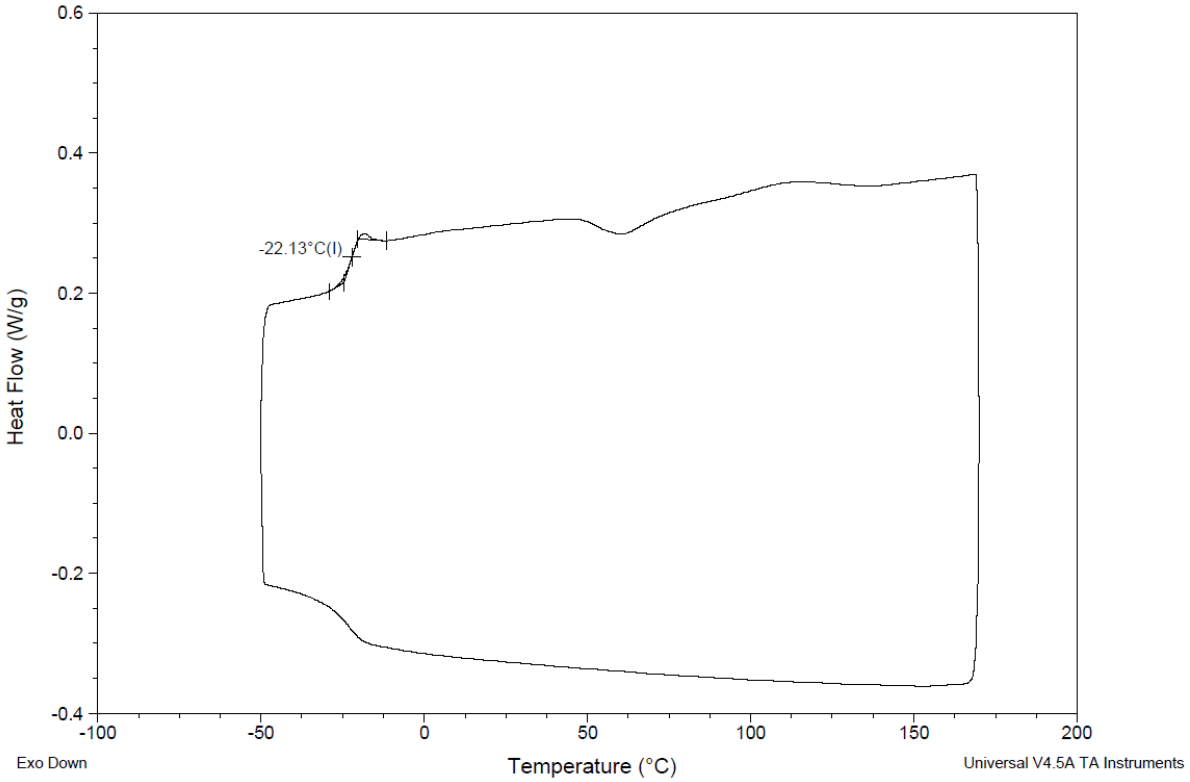

Figure S 46: DSC analysis of BAB[4] (PM/PHB= 77/23; Table 4, Entry 6).

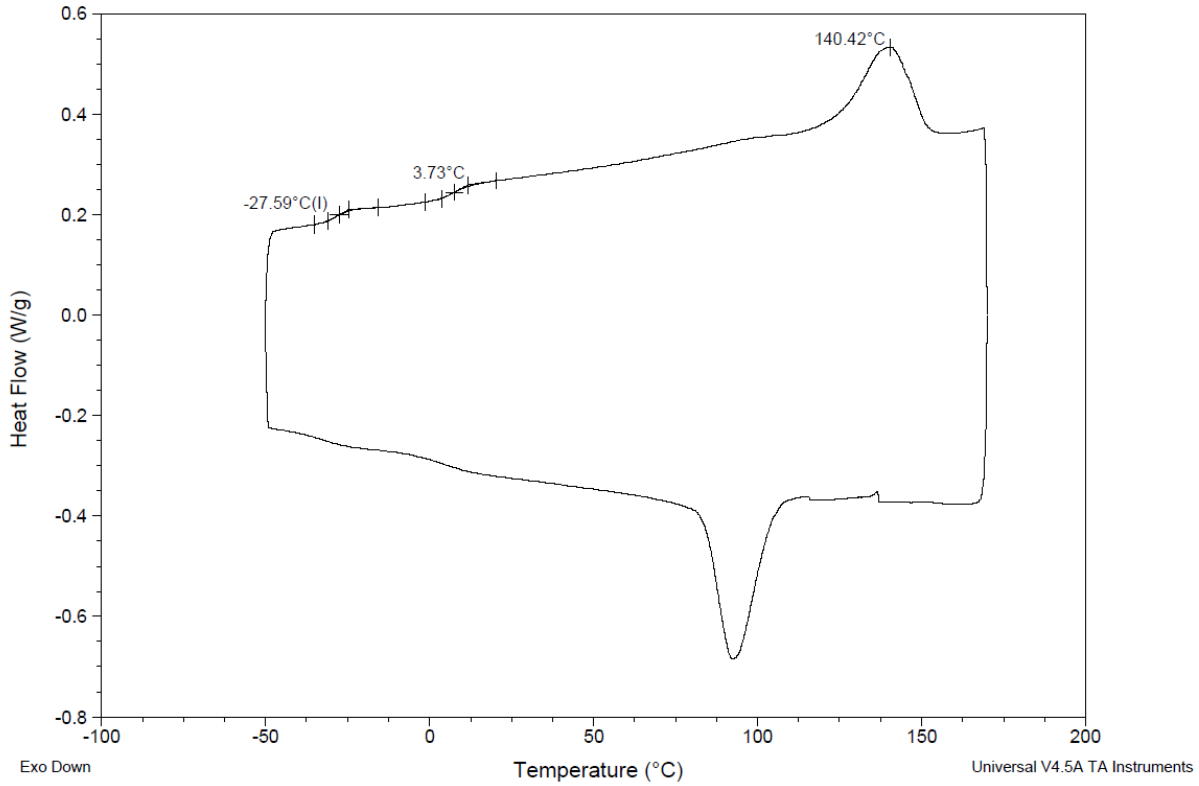

Figure S 47: DSC analysis of a blend from PM (16000 g/mol) and PHB (P_r = 0.85 and M_n = 18000 g/mol).

10) Powder-XRD

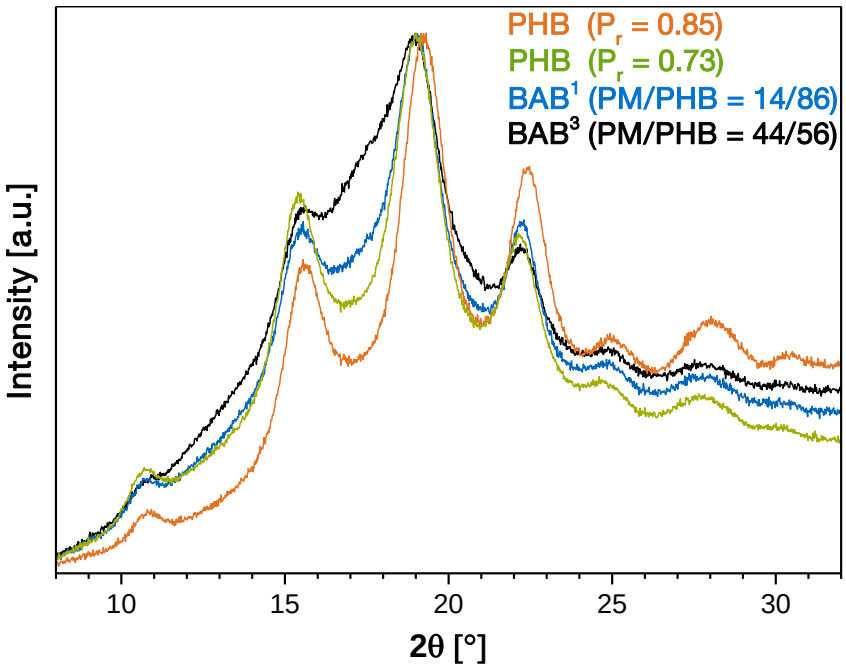

Figure S 48: Powder XRD measurements without background correction of PHB (orange, P_r = 0.85; Table 1, Entry 4), PHB (green, P_r = 0.73; Table 2, Entry 9), BAB^1 (blue, P_r = 0.73; Table 4, Entry 3) and BAB^3 (black, P_r = 0.73; Table 4, Entry 5).

11) SAXS data analysis

Data analysis was performed by fitting the SAXS curves with structural models. The most suiting models are shown below.

1) Pure PHB

The SAXS data of the pure PHB sample were fitted by:

$$I(q) = I_{\text{Porod}}(q) + I_{\text{bg}} \qquad \text{(Eq. 1)}$$

with I_{bg} denoting the constant background and $I_{\text{Porod}}(q)$ being defined as follows with $I_{0,\text{Porod}}$ being the amplitude of this term and a the Porod exponent.[20]

$$I(q)_{\text{Porod}} = \frac{I_{0,\text{Porod}}}{q^a} \qquad \text{(Eq. 2)}$$

2) BAB^{1,3} block copolymers

The SAXS data of the BAB block copolymer samples BAB^1 and BAB^3 were fitted by:

$$I(q) = I_{\text{Porod}}(q) + P_{\text{ell}}(q)\, S_{\text{HS}}(q) + I_{\text{bg}} \qquad \text{(Eq. 3)}$$

$P_{ell}(q)$ is the form factor of an ellipsoid (see below) and $S_{HS}(q)$ the hard-sphere structure factor (see below). The form factor of an ellipsoid reads:[21]

$$P_{ell}(q) = \frac{I_{0,ell}}{V} \int_0^{\frac{\pi}{2}} F(q)^2 sin\theta d\theta \quad \text{(Eq. 4)}$$

$$F(q) = 3\,\frac{(\Delta\rho)V(\sin[qr(a,b,\theta)] - qr\cos[qr(a,b,\theta)])}{[qr(a,b,\theta)]^3} \quad \text{(Eq. 5)}$$

$$r(a, b, \theta) = (b^2 sin^2\theta + a^2 cos^2\theta)^{1/2} \quad \text{(Eq. 6)}$$

Here, $\Delta\rho$ is the difference of scattering length densities between the ellipsoids and the environment, V the ellipsoid volume, a the radius along the rotational axis (polar axis), b the radius perpendicular to the rotational axis (equatorial axis),and θ the angle between the axis of the ellipsoid and the scattering vector $\vec{q}$. The hard-sphere structure factor reads: [22]

$$S_{HS}(q) = \frac{1}{1 + 24\eta G(2R_{HS}q)/(2R_{HS}q)} \quad \text{(Eq. 7)}$$

$$G(x) = \gamma\,\frac{\sin x - x\cos x}{x^2} + \delta\,\frac{2x\sin x + (2 - x^2)\cos x - 2}{x^3} + \varepsilon\,\frac{-x^4\cos x + 4(3x^2 - 6\cos x + (x^3 - 6x)\sin x + 6)}{x^5} \quad \text{(Eq. 8)}$$

The used functions γ, δ and ε are defined as follows:

$$\gamma = \frac{(1 + 2\eta)^2}{(1 - \eta)^4} \quad \text{(Eq. 9)}$$

$$\delta = \frac{-6\eta\left(1 + \frac{\eta}{2}\right)^2}{(1 - \eta)^4} \quad \text{(Eq. 10)}$$

$$\varepsilon = \frac{\gamma\eta}{2} \quad \text{(Eq. 11)}$$

The parameter η is the hard-sphere volume fraction, which is the volume fraction that is occupied by the correlated particles per unit detection volume, and $S_{HS}(q)$ is defined as half the distance between two particles. [23]

The resulting values of the fitting parameters are listed in Table S1.

Table S1: Analysis results from model fitting of SAXS plots for PHB, BAB[1] and BAB[3]

Sample	**PHB** ($P_r = 0.85$)	**BAB[1]** (PM/PHB = 14/86)	**BAB[3]** (PM/PHB = 44/56)
Porod term, α	4.02 ± 0.003	4.13 ± 0.005	3.98 ± 0.02
Ellipsoid form factor	-	a = 3.4 ± 0.8 nm b = 7.4 ± 2.2 nm	a = 4.1 ± 1.3 nm b = 8.0 ± 1.4 nm
Hard-Sphere structure factor	-	R_{HS} = 9.1 ± 0.9 nm η = 0.11 ±0.005	R_{HS} = 9.5 ± 2.5 nm η = 0.20 ± 0.002

12) Hot-Molding

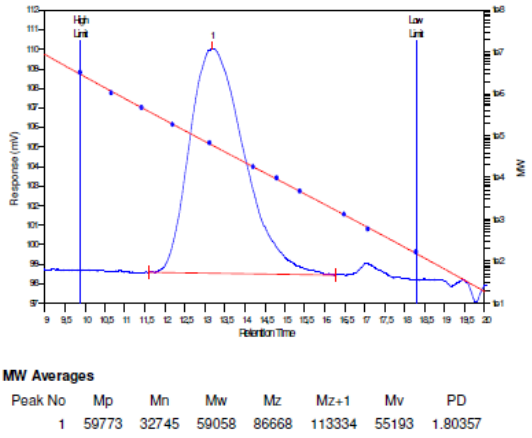

MW Averages

Peak No	Mp	Mn	Mw	Mz	Mz+1	Mv	PD
1	59773	32745	59058	86668	113334	55193	1.80357

Figure S 49: SEC trace in chloroform of PHB produced with catalyst 1 (Table 2, Entry 3) after hot molding.

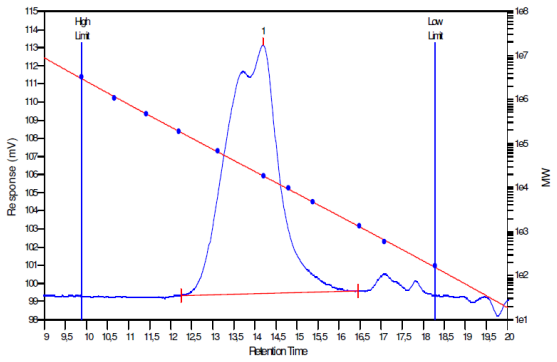

MW Averages

Peak No	Mp	Mn	Mw	Mz	Mz+1	Mv	PD
1	18397	19219	30066	42952	56604	28345	1.56439

Figure S 50: SEC trace in chloroform of BAB[3] produced with catalyst 4 (Table 4, Entry 5) after hot molding.

13) Mechanism elucidation

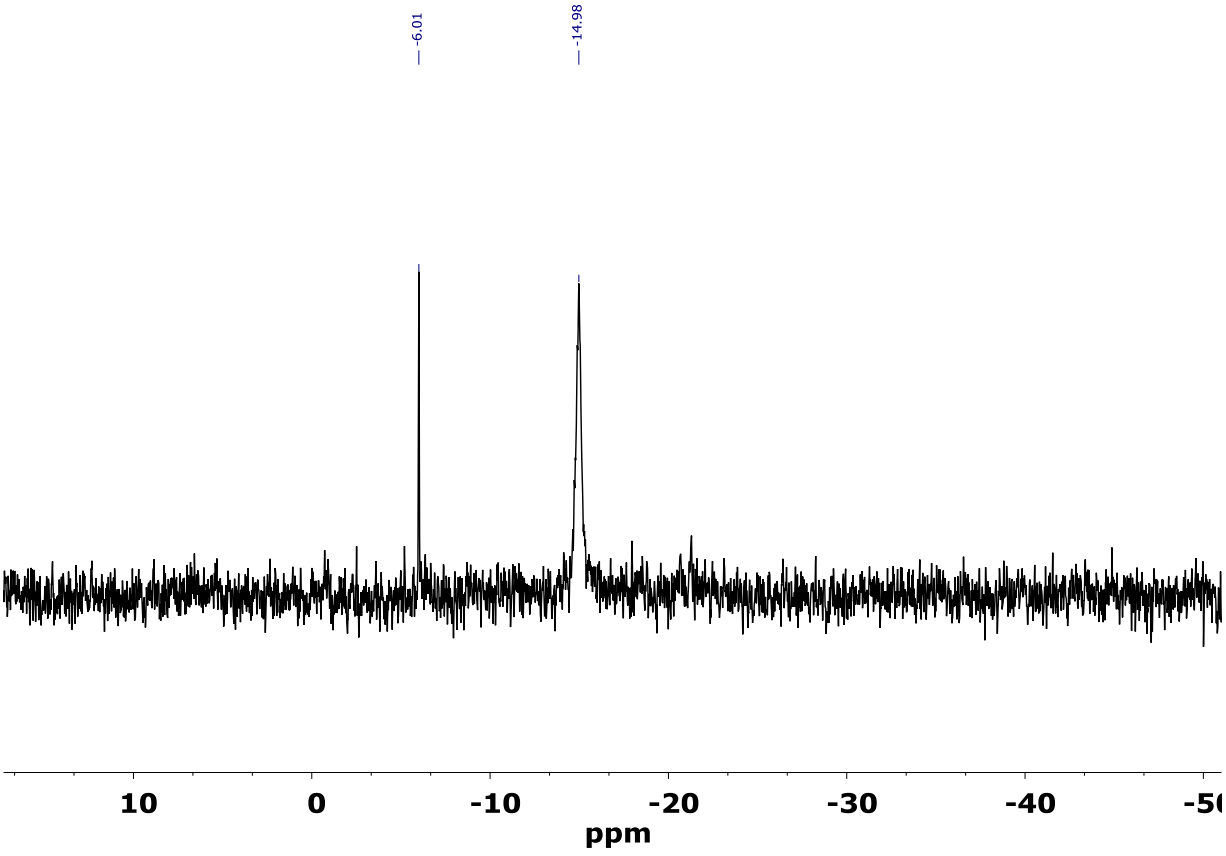

Figure S 51: ^{31}P NMR spectrum in C_6D_6 obtained after addition of excess of $(PhO)_2POCl$ (δ = -6.01) to the polymerization reaction mixture of menthide and catalyst 4 in C_6D_6.

14) References

[1] G. A. Olah, A. Goeppert, G. K. S. Prakash, *J. Org. Chem.* **2009**, *74*, 487-498.

[2] H. Koempel, W. Liebner, in *Studies in Surface Science and Catalysis, Vol. 167* (Eds.: F. Bellot Noronha, M. Schmal, E. Falabella Sousa-Aguiar), Elsevier, **2007**, pp. 261-267.

[3] X. Zuwei, Z. Ning, S. Yu, L. Kunlan, *Science* **2001**, *292*, 1139-1141.

[4] E. E. Stangland, K. B. Stavens, R. P. Andres, W. N. Delgass, *J. Catal.* **2000**, *191*, 332-347.

[5] T. Hayashi, K. Tanaka, M. Haruta, *J. Catal.* **1998**, *178*, 566-575.

[6] V. Russo, R. Tesser, E. Santacesaria, M. Di Serio, *Ind. Eng. Chem. Res.* **2013**, *52*, 1168-1178.

[7] V. Mahadevan, Y. D. Y. L. Getzler, G. W. Coates, *Angew. Chem. Int. Ed.* **2002**, *114*, 2905-2908.

[8] J. T. Lee, P. J. Thomas, H. Alper, *J. Org. Chem.* **2001**, *66*, 5424-5426.

[9] S. O. Nwaukwa, P. M. Keehn, *Tetrahedron Lett.* **1982**, *23*, 35-38.

[10] D. Zhang, M. A. Hillmyer, W. B. Tolman, *Biomacromolecules* **2005**, *6*, 2091-2095.

[11] J. Shin, M. T. Martello, M. Shrestha, J. E. Wissinger, W. B. Tolman, M. A. Hillmyer, *Macromolecules* **2011**, *44*, 87-94.

[12] K. C. Hultzsch, P. Voth, K. Beckerle, T. P. Spaniol, J. Okuda, *Organometallics* **2000**, *19*, 228-243.

[13] E. Y. Tshuva, S. Groysman, I. Goldberg, M. Kol, Z. Goldschmidt, *Organometallics* **2002**, *21*, 662-670.

[14] P. T. Altenbuchner, B. S. Soller, S. Kissling, T. Bachmann, A. Kronast, S. I. Vagin, B. Rieger, *Macromolecules* **2014**, *47*, 7742-7749.

[15] C.-X. Cai, L. Toupet, C. W. Lehmann, J.-F. Carpentier, *J. Organomet. Chem.* **2003**, *683*, 131-136.

[16] F. Adams, M. R. Machat, P. T. Altenbuchner, J. Ehrmaier, A. Pothig, T. N. V. Karsili, B. Rieger, *Inorg. Chem.* **2017**, *56*, 9754-9764.

[17] F. Adams, M. Pschenitza, B. Rieger, *ChemCatChem* **2018**, *0*.

[18] P. T. Altenbuchner, P. D. Werz, P. Schöppner, F. Adams, A. Kronast, C. Schwarzenböck, A. Pöthig, C. Jandl, M. Haslbeck, B. Rieger, *Chem. Eur. J.* **2016**, *22*, 14576-14584.

[19] N. Ajellal, M. Bouyahyi, A. Amgoune, C. M. Thomas, A. Bondon, I. Pillin, Y. Grohens, J.-F. Carpentier, *Macromolecules* **2009**, *42*, 987-993.

[20] G. Porod, *Kolloid-Zeitschrift* **1952**, *125*, 51-57.

[21] A. Isihara, *The Journal of Chemical Physics* **1950**, *18*, 1446-1449.

[22] L. Feigin, D. I. Svergun, *Structure analysis by small-angle X-ray and neutron scattering, Vol. 1*, Springer, **1987**.

[23] J. K. Percus, G. J. Yevick, *Physical Review* **1958**, *110*, 1-13.